Food and Chemical Toxicology 156 (2021) 112435

Contents lists available at ScienceDirect

Food and Chemical Toxicology

journal homepage: www.elsevier.com/locate/foodchemtox

Proteomic profile of the effects of low-dose bisphenol A on zebrafish ovaries

Ana M. Molina [a,1], Nieves Abril [b,1,*], Antonio J. Lora [**,a], Paula V. Huertas-Abril [b], Nahum Ayala [a,2], Carmen Blanco [a], M.Rosario Moyano [a,2]

[a] Departamento de Anatomía y Anatomía Patológica Comparadas y Toxicología. Facultad de Veterinaria. Universidad de Córdoba, Campus de Rabanales, 14014, Córdoba, Spain

[b] Departamento de Bioquímica y Biología Molecular, Campus de Excelencia Internacional Agroalimentario CeiA3, Universidad de Córdoba, Campus de Rabanales, Edificio Severo Ochoa, 14071, Córdoba, Spain

ARTICLE INFO

Handling Editor Dr. Jose Luis Domingo

Keywords:
Bisphenol-A
Ovary
Zebrafish
Proteomic
Proteostasis

ABSTRACT

Human exposure to bisphenol-A (BPA) is largely unavoidable because BPA is an environmental contaminant found in soil, water, food and indoor dust. The safety of authorized BPA amounts in consumer products is under question because new studies have reported adverse effects of BPA at doses far below that previously established by the NOAEL (50 μg/kg per day). To protect public health, the consequences of low-dose BPA exposure in different organs and organismal functions must be further studied to generate relevant data. This study attempted to investigate the effects and potential molecular mechanisms of short-term exposure to 1 μg/L BPA on zebrafish ovarian follicular development. We observed only minor changes at the histopathological level with a small (3 %) increase in follicular atresia. However, a shotgun proteomics approach indicated deep alterations in BPA-exposed ovarian cells, including induction of the oxidative stress response, metabolic shifts and degradome perturbations, which could drive oocytes towards premature maturation. Based on these results, it could be suggested that inadvertent exposure to small concentrations of BPA on a continuous basis causes alteration in biological processes that are essential for healthy reproduction.

1. Introduction

Bisphenol A (BPA, 2,2-bis(4-hydroxyphenyl)propane) is commonly used in the production of polycarbonates and epoxy resins. These materials are employed to line the interior of cans, bottle caps, pipes, and tanks for drinking water and used in the manufacturing of plastic food packages. BPA is also used in the manufacturing of thermal paper, and the recycling streams introduce BPA to recycled carton and paper. Human exposure to this compound is hence, virtually unavoidable because BPA is present in soil, water, food and indoor dust (Murata and Kang, 2018; Russo et al., 2019; Valentino et al., 2016). In fact, most humans have detectable levels of BPA and BPA metabolites in their urine (Calafat et al., 2008), indicating chronic exposure. This study by Calafat analyzed for 6 years more than two thousand participants and detected BPA in 92.6 % of individuals, with total concentrations ranging from 0.4 μg/L to 149 μg/L (Calataf et a., 2008). Metabolic and toxicokinetics studies detected a rapid BPA excretion rate (>90 %) in urine in the first 4–5 h after oral administration of environmental doses of BPA in humans, what means that only a very small percentage of the compound would be available for other biotransformation pathways (Völkel et al., 2002; Andra et al., 2016). However, and despite this fast metabolism, the problem persists since people's exposure to BPA is continuous and inadvertent, being constantly exposed through diet or environmental contamination, among others. Metabolism in rodents is not so fast (Völkel et al., 2002). However, hundreds of human epidemiology and controlled laboratory animal studies have demonstrated the adverse health outcome association between BPA exposure and human diseases (Valentino et al., 2016), including metabolic disorders. The similarity of the phenol groups of both BPA and estradiol enables BPA to exert weak estrogenic activities because it is considered an endocrine disrupter

* Corresponding author. Departamento de Bioquímica y Biología Molecular, Campus de Excelencia Internacional Agroalimentario CeiA3, Universidad de Córdoba, Campus de Rabanales, Edificio Severo Ochoa, 14071, Córdoba, Spain.

** Corresponding author. Departamento de Anatomía y Anatomía Patológica Comparadas y Toxicología. Facultad de Veterinaria. Universidad de Córdoba, Campus de Rabanales, 14014, Córdoba, Spain.

E-mail addresses: bb1abdim@uco.es (N. Abril), v12lobea@uco.es (A.J. Lora).

[1] Both authors, AMML and NAD, contributed equally to this manuscript and should be considered as first author.

[2] Both authors contributed equally to this work and share senior authorship.

https://doi.org/10.1016/j.fct.2021.112435

Received 19 March 2021; Received in revised form 7 July 2021; Accepted 18 July 2021

Available online 21 July 2021

(ED), which triggers estrogenic pathways in the body, and has an impact on human fertility, thus causing reproductive pathologies and decreased fertility [reviewed in (Matuszczak et al., 2019)].

In a 2015 EFSA (European Food Safety Authority) report, an exhaustive evaluation of the effects of BPA on the health of the human population was made in three different ways: (1) external (by diet, drinking water, inhalation, and dermal contact to cosmetics and thermal paper); (2) internal exposure to total BPA (absorbed dose of BPA, sum of conjugated and unconjugated BPA); and (3) aggregated (from diet, dust, cosmetics and thermal paper). Based on the results of the different studies analyzed, the panel of experts estimated that there were no health problems for any age group due to dietary exposure and a low health risk from added exposure. However, the panel of experts observed considerable uncertainty in the exposure estimates for non-dietary sources and indicated the necessity of additional studies. The EFSA report is continuously re-evaluating the public health risks related to the presence of BPA in food. In January 2018, the European Parliament's Committee on the Environment, Public Health and Food Safety approved the EFSA commission's proposal to reduce the specific migration limit applicable to plastics, coatings and varnishes from 0.6 mg/kg to 0.05 mg/kg (Regulation, 2011/10; Regulation, 2018/213). A ban was also imposed on the presence of BPA in plastic bottles and containers for food for babies and children under three years of age. Since January 2020, the commercialization or use of thermal paper with a concentration equal to or greater than 0.02 % has been prohibited in the EU (Regulation, 2016/2235).

Regulation of chemicals is based on the premise that higher concentrations of a chemical will have more significant toxic effects, which are designated in terms of the LD_{50} (dose that kills 50 % of the test animals), MTD (maximum tolerated dose), LOAEL (dose that produces the lowest observed adverse effect) or NOAEL (No Observed Adverse Effect Level). However, strong controversy is observed about the safe amounts of BPA that can be used in consumer products. The Consortium Linking Academic and Regulatory Insights on BPA Toxicity (CLARITY-BPA, https://onlinelibrary.wiley.com/doi/full/10.1111/bcpt.13125) has recently presented the results of a study conducted by the FDA's National Center for Toxicological Research (NCTR) aimed to investigate the full range of human health effects of BPA. The study involved oral gavage treatment of rats with BPA at doses of 2.5–25 μg/kg-bw/day, and analyses were performed on one sample pool of animals and tissues by multiple laboratories (Badding et al., 2019). The results showed adverse effects of BPA at low doses (2.5 μg/kg per day), which were far below the previously established NOAEL (50 μg/kg per day) or the tolerable daily intake (TDI; 4 μg/kg per day) established by the EFSA in 2015 (Prins et al., 2018). BPA is a known endocrine-disrupting chemical (EDC) that can mimic the body's hormones and estrogen. The expression of estrogen receptors varies in different tissues; hence, to produce data that can be used to protect public health, it is imperative to continue analyzing the consequences of low-dose BPA exposure in each organ. Several findings suggest that BPA also acts in other ways in addition to via estrogen receptors, including oxidative stress, DNA damage, epigenetic modifications, and biological processes that are essential for early embryonic development (Guo et al., 2017; Patel et al., 2017) and healthy reproduction.

To gain insights into the molecular mechanisms of BPA toxicity, we carried out a shotgun proteomic analysis to characterize the biological responses elicited by a low dose (1 μg/L) of this ED chemical (EDC) in the ovary of zebrafish (*Danio rerio*). Zebrafish is a small fish (~3 cm long) native to streams in India that successfully emerged as a major model organism for the study of vertebrate development and physiology. This teleost fish has also been extensively used to investigate the mode of action of EDCs and their effects on reproduction. Findings obtained in this model species can be extrapolated to other vertebrates because of the similarity of their endocrine system at the molecular level (Li et al., 2019; Segner, 2009), specially because the ability of zebrafisfh to fast metabolizing BPA (Lindholst et al., 2003) as described for humans.

Numerous studies have shown that BPA has the potential to impact different stages of oocyte development by disrupting early oogenesis, promoting the transition of primordial follicles to primary follicles and suppressing the meiotic maturation of oocytes due to abnormal spindle assembly during meiosis I [Migliaccio et al., 2018a and references herein]. In a previous work, we evaluated the short-term effects of different BPA doses on follicular development in *D. rerio*. The histological evaluation of the ovaries revealed a dose-related increase in the proportion of follicular atresia affecting the different types of follicles. The whole-body vitellogenin (VTG) concentration significantly increased in a dose-dependent manner, reaching a 12-fold increase at the highest assayed dose. In contrast, the kinetics of *Cyp19a* transcript abundance variation, which were determined via a quantitative RT-PCR assay, showed a nonmonotonic dose-response curve, with a remarkable decrease in the number of ovarian aromatase *Cyp19a* mRNA molecules at the lowest assayed BPA concentration (1 μg/L), which produced no significant histological changes or total VTG increases (Molina et al., 2018b). Consistently, a similar response was obtained when analyzing the transcript amounts of *Cyp19b* in the brain (Molina et al., 2018a). Since aromatase, a cytochrome P450 superfamily member, catalyzes the synthesis of the steroid hormone 17β-estradiol (E2) from androgens, the depletion of its levels by 1 μg/L BPA exposure may cause profound alterations in the ovary, thereby interfering with correct ovarian functionality.

The proteome is the complement of proteins present in a biological system (living cell, tissue or organism) at any given time. Shotgun proteomics provides a means to qualitatively and quantitatively analyze complex proteomes that does not require prior polyacrylamide gel electrophoresis and protein staining. In this approach, tens of thousands of peptides obtained by in-solution digestion of extracted protein mixtures are fractionated by liquid chromatography (LC) and then identified by MS/MS. Peptide fragment ion MS/MS spectra were used to interrogate protein, gene and transcriptome (RNA-seq) databases, and proteins were identified. Comparisons of proteomes obtained from control and BPA-exposed animals will provide insights on the toxicity of BPA at low doses and the underlying mechanisms, which will help regulators make decisions to protect public health. Hence, the aim of this work was to characterize the direct toxic effects of BPA on proteostasis in the ovary and its possible relationship with disruption of follicular development in the ovary at a low dose (1 μg/L) that does not produce observable changes at the histological level but caused a marked downregulation of ovarian aromatase (Molina et al., 2018b). Our work will contribute to defining molecular biomarkers for the early detection of environmental BPA exposure and identifying safe BPA amounts for use in consumer products.

2. Materials and Methods

2.1. Animals, BPA exposure and sampling

Forty-two female zebrafish (*Danio rerio*) in the last stage of their juvenile period (16 weeks old) (Singleman and Holtzman, 2014) were randomly distributed into two groups. The experimental group was exposed to 1 μg/L BPA (Sigma-Aldrich®) for 14 days. The water quality parameters were controlled during the study. The control group was maintained under similar conditions without contact with the pollutant (The experimental procedure is indicated in the Suppl. Inf. Methods 1). An overdose of tricaine methanesulfonate (MS-222® 500 mg/L; Sigma-Aldrich) buffered with sodium bicarbonate (300 mg/L; Sigma-Aldrich) was used to euthanize the fish. The ovaries of six animals per group were excised, paraffin fixed and used for histological analysis. The other six fish were used for analytical BPA determinations. The ovaries of the last nine fish per group were cryo-homogenized, stored at −80 °C and used for biomolecule extraction (Suppl. Fig. 1 presents the experimental flow). All the experimental procedures were performed at

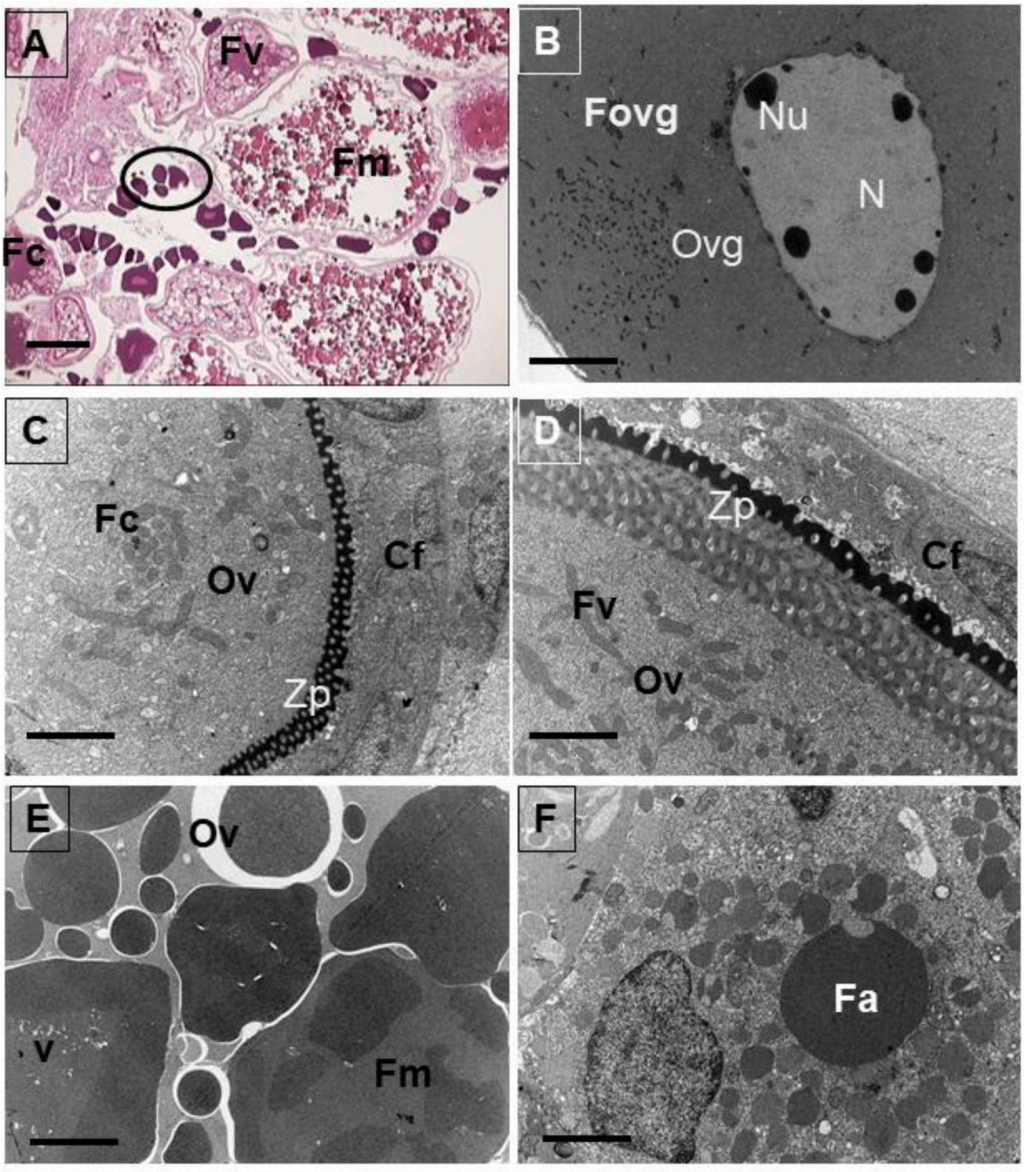

Fig. 1. Zebrafish ovary. A: Light microscopy. Bar: 100 μm. **B, C, D, E, F: Electron microscopy. Bar: 10 μm. A.** Detail of the ovary showing different follicles with typical appearance where it can be indicated the different types of follicles showing a normal structure. Detail of primordial follicles (arrow), cortical alveolar follicles (Fc), vitellogenic follicle (Fv) and mature follicles (Fm). **B.** Primordial follicles with oogonia (**Fovg**), highlighting the ovule (**Ov**) with a homogeneous nucleus (**N**), abundant nucleoli (**Nu**), and homogeneous and dense cytoplasm. **C.** View of cortical alveolar follicles (**Fc**) with normal ovules (**Ov**), pellucid zones (**Zp**) and follicular cells (**Cf**). **D.** Vitellogenic follicle (**Fv**) with an apparently normal ovule (**Ov**), pellucid zone (**Zp**) and follicular cells (**Cf**). **E.** Mature Follicles (**Fm**) detail. The ovule is highlighted (**Ov**), and apparently normal vitellogenic granules (**V**) are shown. **F.** Atretic follicle (**Fa**) showing an apparently normal structure.

the Experimental Animal Service of the University of Córdoba and followed European Regulations for the Protection of Experimental Animals (Directive, 2010/63/EU).

2.2. Quantification of BPA in fish whole-body homogenates

Fish bodies (n = 6 per group) were homogenized in 2 vol of 50 mM Tris-HCl pH 7.4 by using a Ribolyser Sample Homogenizer (Bio-Rad), and the BPA concentration was determined by LC-MS/MS as previously described (Molina et al., 2013) (Suppl. Inf. Methods 2).

2.3. Histological analysis: light and electron microscopy

Ovaries from six animals per group were used for the morphological study using structural, ultrastructural and morphometric key tools previously described by Molina et al. (2013). To avoid interindividual variations, all samples were evaluated by the same operator.

For light microscopy (structural study), samples were routinely processed, sections of 4 μm were mounted and stained with hematoxylin and eosin and used for morphological evaluation. For the transmission electron microscopy (TEM) ultrastructural study, samples were fixed in 2 % glutaraldehyde solution in 0.1 M phosphate buffer (pH 7.4) overnight at 4 °C and the fragments were dehydrated in an ascending acetone series, embedded in resin and routinely processed. Sections were cut on an LKB ultramicrotome at the Central Microscopy Research Facilities of the University of Córdoba. Ultrathin sections were contrasted with uranyl acetate and lead citrate and examined under a JEOL electron microscope (JEM -100CX II). For the morphometric study, the samples were stained with hematoxylin and eosin, and each microscopic image was processed using Visilog 5® software (Noesis). Quantification was performed in a blind manner by an observer experienced in the use of the analysis system (J.G.M.). The system was initially and regularly calibrated using a millimeter slide (Suppl. Inf. Methods 3).

2.4. Proteomic analysis

2.4.1. Protein isolation

Samples of individually cryo-homogenized ovary tissue from the nine zebrafish included in the control or the BPA groups were randomly distributed in four lots (n = 2–3), and four pools were prepared, each containing 50 mg of the frozen ovary from each animal. Pools were homogenized in 3 mL/g of 20 mM phosphate buffer (pH 7.0) containing

10 mM NaCl, 10 mM KCl and 0.1 μL of protease inhibitor cocktail (P2714, Sigma) per μL and centrifuged (14,000×*g*, 10 min, 5 °C; Avanti 30, Beckman®). Nucleotides were removed by mixing the supernatant with 500 U/mL benzonase (E8263, Sigma) for 30 min at room temperature (RT). Mixtures were ultracentrifuged (105,000×*g*, 60 min, 5 °C; Optima TLX, Beckman®), and soluble protein extracts were aliquoted and stored at −80 °C until use. Protein concentrations were determined by using the Bradford method (Bradford, 1976).

2.4.2. Sample preparation for proteomic analysis

Sample preparation and protein analysis were carried out at the Proteomics Facility of the Research Support Central Service, University of Cordoba. Protein extracts were cleaned-up by one-dimensional SDS-polyacrylamide gel electrophoresis (1D SDS-PAGE, 10 % polyacrylamide). Four biological replicates were used for each experimental condition.

Fifty micrograms of protein extract were loaded onto a conventional SDS-PAGE gel (0.75 mm thick, 4 % stacking, and 10 % resolving), and a voltage of 100 V was applied. Then, the run was stopped when the protein extract had entered the resolving gel by 1 cm so that the whole proteome became concentrated in the stacking/resolving gel interface. The gel was then stained with Coomassie brilliant blue R-250 (BioRad), and the protein bands were excised, diced and kept in water.

Gel dices were destained in 200 mM ammonium bicarbonate (AB)/50 % acetonitrile (ACN) for 15 min and then in 100 % acetonitrile for 5 min. Disulfide bonds in protein cysteinyl residues were reduced with 20 mM DTT (dithiothreitol) in 25 mM AB for 20 min at 55 °C. After cooling the samples to room temperature (RT), the free thiol groups were alkylated with 40 mM iodoacetamide in 25 mM AB in the dark for 20 min, after which the gel pieces were washed twice in 25 mM AB and digested in situ with sequencing grade trypsin (Promega, Madison, WI) (2.5 ng/μl of enzyme in 25 mM AB, 37 °C, overnight). Protein digestion was stopped by the addition of 1 % trifluoroacetic acid (final concentration), and the digested samples were SpeedVac dried.

2.4.3. nLC-MS^2 analysis

The digested samples were first trapped in a 5 mm × 0.3 mm pre-column Acclaim Pepmap C18 (Thermo Fisher Scientific) (2 % acetonitrile/0.05 % TFA, 5 min, 5 μl/min). Then, a Dionex Ultimate 3000 nano UHPLC system (Thermo Fisher Scientific) with an Acclaim Pepmap C18 separation column, 500 mm × 0.075 mm, 2-μm pore size (Thermo Fisher Scientific) was used for nLC-MS2 analysis. For peptide separation, mobile phase buffers A and B were composed of water/0.1 % formic acid and 20 % acetonitrile/0.1 % formic acid, respectively. Samples were separated at 300 nL/min and 40 °C. Mobile phase B increased from 4 to 35 % during the first 60 min, then from 35 to 55 % over 3 min and finally from 55 to 90 % over the last 3 min. Samples were washed for 8 min in buffer B and re-equilibrated for 12 min at 4 % buffer B.

A nanoelectrospray ionization interface coupled to the UHLPC converted the eluted peptides into gas-phase ions that were analyzed in an Orbitrap Fusion mass spectrometer (quadrupole-Orbitrap-quadrupole ion trap, Q-OT-qIT; Thermo Fisher Scientific) operated in positive mode. Peptides were detected in survey scans from 400 to 1500 m/z, with the Orbitrap resolution set at 120 K (at 200 m/z) and a 4×10^5 ion count target. MS^2 spectra were acquired with an isolation window of 1.2 m/z using CID (collision-induced dissociation) fragmentation with a normalized collision energy of 35 and rapid scan MS analysis in the ion trap. The AGC (automatic gain control) ion count target was set to 2×10^3, and the maximum ion injection time was 300 ms. Only parent ions with a charge state from 2 to 5 were selected for MS^2. Dynamic exclusion was set for 10 ppm tolerance around the selected precursor and its isotopes, and the exclusion duration was 15 s. Monoisotopic precursor selection was enabled. The instrument was run in top speed mode with 3 s cycles.

2.4.4. MS^2 data analysis

Following MS^2 data acquisition, raw files were processed with MaxQuant software v. 1.5.7.4 (Tyanova et al., 2016a) without performing charge state deconvolution or deisotoping. The search engine Andromeda integrated into MaxQuant was used to interrogate the *Danio rerio* TrEMBL database downloaded from www.uniprot.org (Oct 2018) (62,078 entries). MS^2 spectra were searched with a search precursor mass tolerance of 10 ppm. The fragment tolerance was set to 0.6 Da, and a maximum of one missed cleavage was allowed. Cysteine carbamidomethylation was set as a fixed modification, and methionine oxidation was set as a variable modification. A target-decoy search strategy (TDS) was used to estimate the false discovery rate (FDR). Peptides were validated by filtering at a 1 % FDR *q*-value. Peptide identifications were grouped into protein hits using a simple parsimony algorithm.

2.4.5. Label-free protein quantification

The MaxLFQ algorithms (Cox et al., 2014), which are part of the MaxQuant software suite, were used for label-free protein quantification, and they apply a retention time alignment and enable the "match-between-runs" feature among the replicates of every experimental condition to improve the identifications. All downstream analyses to identify differentially expressed proteins were performed using Perseus software v 1.5.6.0 (Tyanova et al., 2016b), which is freely available from the MaxQuant website (http://www.coxdocs.org/doku.php?id = perseus:start).

Quantification was performed via MaxQuant's LFQ (label-free quantification) algorithm, which combines and adjusts peak areas obtained by the MaxQuant analysis of the ion chromatograms extracted from each fragment of each peptide around the predicted retention time into a protein intensity value (Table S2). Data were normalized according to the median, and LFQ normalized intensity values were log2 transformed. Only proteins identified in at least three replicates per condition were used. Missing values were replaced (imputed) with the value of the lowest intensity. Statistical significance of the protein abundance variations caused by BPA exposure was determined by a two-sample Student's *t*-test with the Benjamini–Hochberg correction (Benjamini and Hochberg, 1995), which fixed an adjusted p-value < 0.05 for the FDR. The results were then filtered, and only proteins with an adjusted p-value < 0.01 and a fold change ≥ 2 were considered.

2.4.6. Interaction network and pathway analysis

Ingenuity pathway analysis (IPA) software was used to map significantly regulated proteins into canonical pathways. To compare the two experimental group ovary samples, the common proteins differentially regulated between the control and BPA-exposed animals were combined with the proteins uniquely expressed in either of the groups, and the overall protein list was uploaded for IPA core analysis using default values. The canonical pathways with a p-value less than 0.05 and z-values greater than 2 or less than −2 were selected as significantly activated or deactivated pathways, respectively. In the IPA "canonical pathway" analysis, the top 10 pathways ranked by p-value were reported. A thorough analysis of the literature was also made for the distribution in functional categories of proteins with altered abundance after exposure to BPA.

3. Results and discussion

BPA is a constituent of many plastics, including those used in can liners and food containers. Hundreds of studies have demonstrated that BPA may adversely affect humans. BPA is rapidly metabolized and it affects metabolism, and the reproductive system because of its estrogenic, antiandrogenic, and antithyroid activities (Rochester, 2013; Matuszczak et al., 2019). Similar to many other endocrine disrupter chemicals (EDCs), bisphenol-A (BPA) induces unconventional non-monotonic dose response (NMDR) relationships (Molina et al., 2018a, 2018b) (Vandenberg, 2014), which have great implications in risk

assessment. BPA effects have been described at doses that are considered low and below those used in traditional toxicological studies (100 pM-1 nM for *in vitro* studies and 25–100 ng/kg for animal models) (Vandenberg, 2014). In this study, we exposed female zebrafish to 1 μg/L BPA for fourteen days and analyzed the consequences on ovarian proteostasis through a shotgun proteomic approach. The rationale for this dose selection was its ability to markedly downregulate the transcript counts of the gene Cyp19a in the ovary of *D. rerio*, as we observed in previous work (Molina et al., 2013, 2018a, 2018b). This enzyme catalyzes the final step in the biosynthesis of estrogens, and its downregulation can be assumed to have important effects on female sexual development and ovarian differentiation and functionality. The proteomic approach used here could enable the identification of potential proteins and molecular networks modified by a low BPA dose in the process of follicular maturation and affect the reproductive potential of females by reducing the quality of the eggs and increasing the atretic follicle percentage.

The experimental procedure did not cause mortality or macroscopic alterations in the animals, and no differences in size or body weight were detected in the treatment group that showed an average wet weight of 0.61 ± 0.09 g and length of 4.07 ± 0.18 cm. Nondetected BPA levels were found in the whole body of animals included in the control group, although a concentration of 0.047 ± 0.005 μg/g ($p < 0.05$) was measured in BPA-exposed zebrafish. A concentration in the range of 0.024–1.427 μg/g was detected in hair samples from a general human population from Seville, Spain (Martín et al., 2019).

3.1. Histological analysis

The reproductive cycle of zebrafish starts when a fraction of oogonia enters mitosis for renewal or meiosis, and they transform to oocytes that develop inside the ovarian follicles in response to a surge in luteinizing hormone (LH) secretion. Significant growth of the oocyte begins after formation of the ovarian follicle (folliculogenesis) through two defined phases. The previtellogenic follicle phase includes stages I and II, where oocytes are enclosed in a single layer of follicular cells, which have with many nucleoli located initially at the periphery of the cell and moving later to the periphery of the nucleus to form the germinal vesicle. The postvitellogenic phase is characterized by the accumulation of exogenously synthesized vitellogenin during stage III. Vitellogenin enters oocytes by receptor-mediated endocytosis and is processed by lysosomal endopeptidases into smaller yolk protein products that are stored in the cytoplasm to serve as nutrients for embryonic development (Li and Ge, 2020; Lubzens et al., 2010; Patiño and Sullivan, 2002). The process ends with germinal vesicle breakdown, the release of the first polar body (stage IV) and expulsion of the oocyte from the follicles in the process of ovulation (stage V). During the folliculogenesis process, some ovarian follicles lose their integrity and are eliminated as part of a highly regulated process called follicular atresia, which is essential for the maintenance of ovarian homeostasis during the reproductive cycle (González-Kother et al., 2020).

In Fig. 1 (A, B, C, D, E), the normal appearance of the ovarian follicles of zebrafish included in our control group under light and transmission electron microscopy (LM and TEM, respectively) is illustrated. All follicles show a typical appearance, with extensive development and a regular distribution of all elements. Under light microscopy, all types of ovarian follicles stand out. The primordial follicle is the smallest and shows very basophilic oocytes. As it evolves and matures, basophilia is lost and cytoplasmic granulations increase until mature follicle granules are formed. Under TEM, oocytes of the primordial follicles show a very homogeneous cytoplasm due to their enormous number of ribosomes, which causes the basophilia observed with LM. The primary follicle becomes lined with follicular cells, and the pellucid zone, which is very dense in electrons, begins to appear. As the follicles mature, the thickness of the zona pellucida increases until it becomes two bands with different thicknesses and electron densities. The maturing follicle changes all its components into metabolic granules, thereby masking the nucleus, which appears with a low density in all follicles, is active, and shows many very dense nucleoli in the primordial follicles.

Similar images without significant observed variations in relation to those in the control group were obtained for the low-dose BPA-exposed fish (Fig. 2A, B, C, D, E, F). In this study group, we found all the follicle types previously described in the control group: primordial follicles, primary follicles (corticoalveolar follicles), vitellogenic follicles, mature follicles and atretic follicles. All of these types maintain the composition and type of lining cells.

The primordial follicles showed an apparently normal morphology with strong basophilia in their oocytes; however, unlike the control group, they presented a certain vacuolization in the peripheric zone of the oocyte. This type of follicle continues to represent the germinal layer of the ovary. Similarly, the corticoalveolar follicles did not show obvious signs of injury in comparison with the control batch, except for some vacuolization located close to the site of formation of the pellucid zone. Vitellogenic and mature follicles showed a slightly reduced number of vitellogenic vesicles and lipid droplets, although they maintained their normal morphology.

Despite the limited histological variations caused by 1 μg/L BPA exposure, differences were observed in the type-cell counts between both experimental groups, although they were not statistically significant. In the control group, approximately 20 % of the follicles were primary growth follicles (Fovg), 30 % were secondary growth follicles (Fc: cortical alveolar follicles), 30 % were vitellogenic follicles (Fv) and the remaining 20 % were mature follicles (Fm) (Fig. 3A). The percentages of different follicle populations varied in the low-dose BPA-exposed group, with increased percentages of previtellogenic follicles (approximately 26 % Fovg and 34 % Fc) and decreased levels of Fv (28 %) and Fm (12 %).

In addition, the global percentage of atretic follicles increased approximately 3-fold after BPA exposure, with significant differences observed between the control and treated groups ($p < 0.05$) but BPA exposure did not equally affect all types of follicles. Higher relative increases in atresia of 1 % and 1.6 % were observed in the Fovg and Fc populations, respectively (Fig. 3B). These results indicate that low-dose BPA disrupted follicular development at the primary stages, thereby hindering follicle maturation; we proposed this hypothesis for the first time in 2018 (Molina et al., 2018b), and it has since been corroborated by others (Migliaccio et al., 2018b).

3.2. Proteomics study

The complexity of BPA toxicity was addressed in this work by using a shotgun proteomic approach. Shotgun proteomics permits the simultaneous quantification of several hundred proteins and the identification of specific alterations and physiological responses between exposures and controls, allowing a better understanding of the toxicity mechanisms of BPA. We used nLC-MS^2 to separate and identify the ovarian proteins present in each of four biological replicates from the experimental group, i.e., the control group and the 1 μg/L BPA-exposed group. A total of 14,110 peptides with a FDR <0.01 were detected in the eight samples, with an average of 9481 ± 289 peptides per sample. More than 74 % of these peptides were unique peptides present in only one protein of the zebrafish proteome. These peptides confidently identified 3431 proteins and 1502 different protein species. Following data filtration, 523 proteins were significantly differentially expressed (≥2-fold change, $p < 0.01$) between the compared experimental groups. Eighty proteins were detected only in the control group, and 132 were exclusive to the 1 μg/L BPA group (Suppl. Fig. 2). Up to 231 proteins from a total of 311 proteins present in both groups were upregulated while the other 80 proteins were downregulated under BPA exposure (Suppl. Fig. 2).

Differentially expressed proteins were further investigated to reveal the associated biological pathways using the bioinformatic tool QIAGEN's Ingenuity® Pathway Analysis (IPA®, www.qiagen.com/ingenuity). The IPA® program uses scientific information contained in

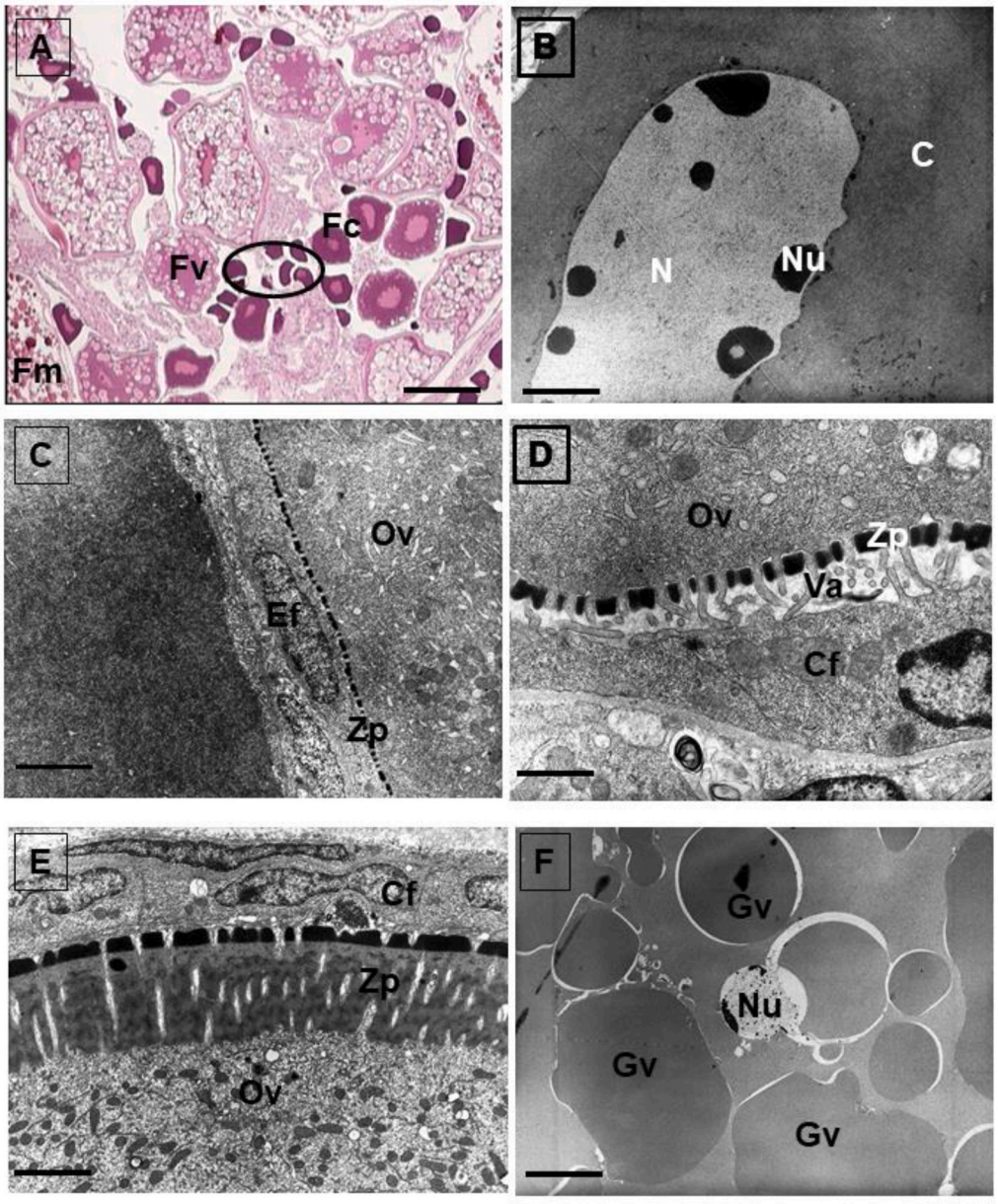

Fig. 2. Zebrafish ovary exposed to 1 μg/L BPA. A: Light microscopy. Bar, 100 μm. **B, C, D, E, F:** Electron microscopy. Bar, 10 μm. **A.** Detail of the ovary where different follicles with typical appearance are shown. Detail of **p**rimordial follicles (arrow), cortical alveolar follicles (Fc), vitellogenic follicle (Fv) and mature follicles (Fm). **B.** Primordial follicle showing the nucleus **(N)** with numerous nucleoli **(Nu)** and homogeneous cytoplasm due to the large number of existing ribosomes. **C.** Detail of a cortical alveolar follicle with the presence of flat follicular epithelium **(Ef)**, oocytes **(Ov)** and zona pellucida **(Zp). D.** Detail of a cortical alveolar follicle where the existence of the pellucid zone **(Zp)** and vacuolizations **(Va)** in the separation with the follicular cell **(Cf)** stand out. **E.** Detail of the vitellogenic follicle showing the double layer of the pellucid zone **(Zp)** lined by polystratified follicular cells **(Cf). F.** Details of vitellogenic granules **(Gv)** in mature follicles.

the Ingenuity Knowledge Base to extract connectivity networks and to generate global canonical pathways displaying the location of analyzed proteins within well-established signaling or metabolic pathways. IPA software found 348 analysis-ready molecules across observations. The top 10 influenced pathways were *glycine betaine degradation*, *SPINK1 pancreatic cancer pathway*, *glycolysis I*, *gluconeogenesis I*, *glutathione-mediated detoxification*, *NRF2-mediated oxidative stress response*, *methionine degradation*, *glutathione redox reactions I*, *cysteine biosynthesis III*, and *epithelial adherent junctions signaling* (Fig. 4A). The significance values (p-value of overlap, i.e., the probability of association of molecules from a dataset with the canonical pathway by random chance alone) for these canonical pathways, calculated by the right-tailed Fisher's exact test, ranged from 2.1×10^{-7} to 6.7×10^{-4}.

Most of these top canonical pathways are partially linked, as we will discuss ahead. For example, glycolysis synthesizes glyceraldehyde 3-phosphate, a precursor for the generation of amino acid serine. Serine then enters the methionine pathway to produce cysteine, leading to GSH production that protects cells from oxidative stress. Cysteine can be converted back to pyruvate by transamination. The glycolysis-to–pentose phosphate pathway generates NADPH, also contributing to counteracting oxidative stress. A thorough review of the literature allowed us to classify the proteins differentially expressed as a result of treatment into 12 wide-ranging functional categories shown in Fig. 4B and Suppl. Table 1.

3.2.1. Low-dose BPA exposure causes oxidative stress response induction and alteration of the one-carbon pathway

The negative effects of oxidative stress on reproduction are undeniable, as is the ability of BPA to generate such oxidative stress (Biswas et al., 2020; Gassman, 2017). However, numerous conflicting reports about BPA prooxidant/antioxidant behavior hinder a better understanding of the mechanisms underlying BPA oxidative homeostasis impairment, which is highly dependent on the dose, the cell type, the tissue, the organ and the biological system employed (Gassman, 2017). Several recent reports integrated data from the current BPA literature and concluded that a wide variety of BPA doses promote reactive oxygen species (ROS) generation and oxidative stress, which induce mitochondrial dysfunction and several cell signaling pathways with fatal

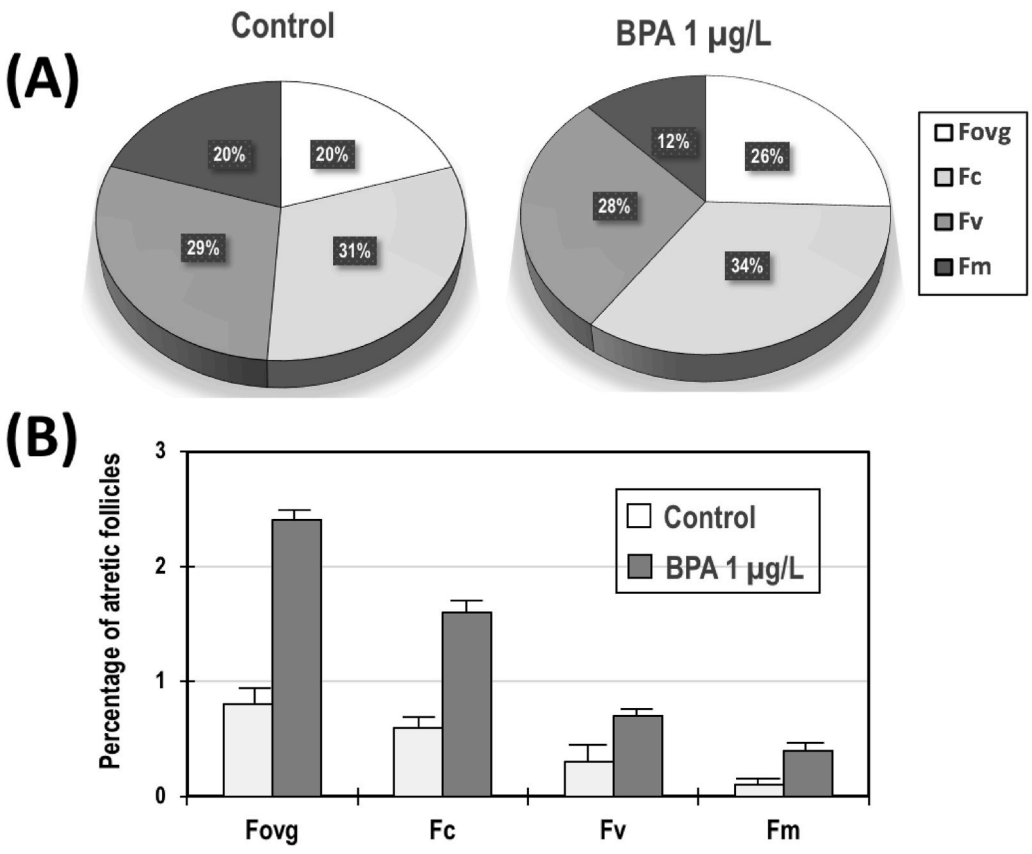

Fig. 3. Quantitative histomorphological assessment of the effect of BPA exposure on follicle development. (A) Percentage of the different types of follicles visualized in the ovaries of control and 1 µg/L BPA-exposed animals. **(B)** Follicular atresia caused by BPA exposure. The percentage of atretic follicles in the different follicular populations in the control and 1 µg/L BPA-exposed groups is presented. **Fovg:** primordial follicles; **Fc:** cortical alveolar follicles; **Fv:** vitellogenic follicles; **Fm:** mature follicles.

pleiotropic effects on general cell function and female reproduction (Meli et al., 2020; Steffensen et al., 2020). Antioxidative defense is achieved by the coordinated actuation of enzymes such as superoxide dismutase (SOD), catalase (CAT), glutathione reductase (GR) and glutathione peroxidase (GPx). Antioxidant enzymes coordinately act with a plethora of antioxidant metabolites (vitamins E and C, reduced glutathione-GSH, carotenoids and flavonoids) that intercept ROS activity. When antioxidant defenses are overwhelmed, ROS cause oxidative damage to proteins, DNA and lipids, including that of the mitochondrial membrane, and the respiratory chain and other critical metabolic pathways are impaired. Nrf2 is the transcription factor that regulates the inducible expression of a battery of approximately 250 genes upon redox perturbation (Tebay et al., 2015). Nrf2-regulated genes encode key components of the glutathione-based and thioredoxin-based antioxidant systems, including CAT, SOD, thioredoxin (TXN), glutaredoxin (GRX) and many other phase I- and phase II-metabolizing enzymes involved in xenobiotic metabolism and detoxification, such as the glutathione-dependent enzymes GPXs, GR and glutathione transferases (GSTs). Our data indicate that 1 µg/L BPA activates the nuclear factor-erythroid 2 p45-related factor 2 (Nrf2)-mediated oxidative stress response. As shown in Suppl. Table 1, more than 40 proteins related to the canonical *NRF2-mediated oxidative stress response pathway* showed changes their relative abundance in the ovaries of BPA-exposed zebrafish. Data (fold-change variations) for some of the proteins included in this class are also shown in Fig. 5. The increased abundance of a so high number of proteins involved in the antioxidative response suggests the ability of 1 µg/L BPA to enhance intracellular ROS generation to levels that elicit the cellular antioxidant response, results that are consistent with previous reports in mice and cell cultures (Berger et al., 2016; Chepelev et al., 2013). The absence of important visible histopathological damage at the studied BPA dose (as shown in Fig. 2) indicates that the elicited ovarian cell antioxidative stress response is effective in neutralizing at least part of the ROS effects. Data in Suppl. Table 1 indicates that other mechanisms assist the Nrf2 response against oxidative stress. Remarkably, the increased levels of hemoglobin (HB) in BPA-exposed ovarian cells (Suppl. Table 1, Fig. 5). The reproductive tract is a low oxygen environment that favors oocyte maturation, in part by activating hypoxia-inducible factor (HIF) target genes. Numerous reports have described the key role of HB in reproductive nonerythroid tissues and other tissues by acting as a potent antioxidant. HB sequesters reactive oxygen species and regulates oxygen concentration, and it has downstream effects on HIF target gene expression, which is critical for the differentiation of the antral follicle after the ovulatory signal (Lim et al., 2019). Overall, data presented here suggest that, under exposure to a low dose of BPA, increases in Nfr2-regulated, HB other stress responses, improve ROS remediation in the follicles, thereby preventing significant histological damage (Fig. 2) despite the generation of oxidative stress, at least at this exposure dose.

The ability of ovarian cells to cope with the toxicity of 1 µg/L BPA was heightened by an increase in the levels of many proteins involved in the one-carbon metabolism, which led to the abundance of GSH by enhanced cysteine, glutamic acid and glycine generation in the *glycine betaine degradation*, *methionine degradation* and *cysteine biosynthesis III* pathways. Fig. 6 integrates these pathways and shows the location of some ovarian proteins deregulated by the low-dose BPA exposure. These three pathways work with the folate and transulfuration pathways in one-carbon metabolism to generate methyl groups utilized in cellular biosynthesis, methylation reactions and cell redox status regulation. Several reports have closely linked one-carbon metabolism to cell transformation and cancer (Newman and Maddocks, 2017; Rizzo et al., 2018). Low-dose BPA treatment increased the abundance of many of the enzymes involved in this metabolic pathway in the zebrafish ovary (Suppl. Table 1). To the best of our knowledge, a conclusive explanation has not been provided regarding how the activation of the metabolism of a carbon contributes to the poor quality of oocytes. However, the scheme in Fig. 6 suggests that activation of one-carbon metabolism

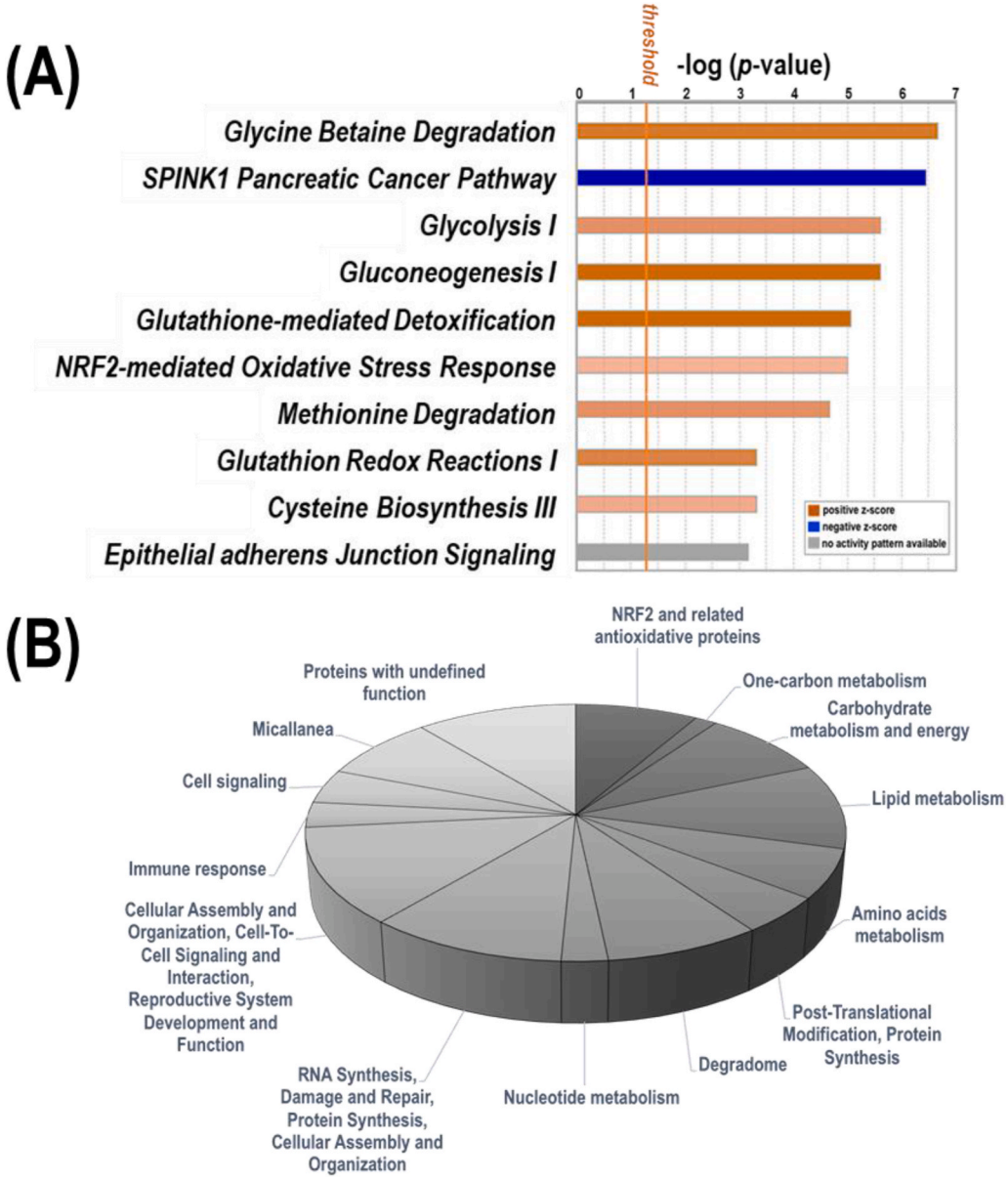

Fig. 4. (A) Top 10 pathways influenced by low-dose BPA (1 μg/L) exposure in the ovary of *Danio rerio*. The significance values (p-value of overlap, i.e., the probability of association of molecules from a dataset with the canonical pathway by random chance alone) for these canonical pathways, calculated by the right-tailed Fisher's exact test, ranged from 2.1×10^{-7} to 6.7×10^{-4}. **(B)** Classification in broad functional categories of the proteins affected by low-dose BPA (1 μg/L) exposure in the ovary of *Danio rerio*.

consumes the cellular amounts of glycine betaine (*N*,*N*,*N*-trimethylglycine), a metabolite with at least two defined roles in oocyte maturation, cell volume regulation and methyl group donors (Lee et al., 2012), which undoubtedly affects oocyte quality. It has also been reported that BPA increases methylation errors in mouse cultured preantral follicles, with detrimental effects on the meiotic process (Trapphoff et al., 2013). Abnormal activation of one-carbon metabolism is also a characteristic trait of some reproductive/endocrine disorders, such as polycystic ovary syndrome (PCO) (Jia et al., 2016) (Xiong et al., 2020). Activation of the one-carbon path increases the levels of homocysteine in follicular fluid, which has been associated with poor oocyte and embryo qualities in PCO patients, and hypermethylation (and downregulation) of mitochondrial genes has been proposed as the causative origin (Jia et al., 2016; Shukla and Mukherjee, 2020; Zhang et al., 2019). According to those reports linking the upregulation of the one-carbon pathway to PCO (Li et al., 2018 and; Maleedhu et al., 2014) ovarian cancer (Nunes et al., 2018; Zhu et al., 2018), our data suggest that inadvertent exposure to small concentrations of BPA on a continuous basis may influence the occurrence of ovarian cancer in the long term through deregulation of DNA methylation patterns as reported for human ovarian carcinoma cell lines (Shi et al., 2017; Hui et al., 2018). Further studies are needed to confirm this hypothesis.

3.2.2. *BPA exposure alters glucose metabolism*

Some of the upregulated Nrf2-and HIF-responsive proteins are involved in NADPH generation, lipid metabolism, and glucose/glycogen metabolism (Ryoo and Kwak, 2018), and their activation could improve cellular metabolic regulation and oocyte developmental competence. Indeed, Fig. 6 suggests that activation of the one-carbon metabolism is linked to the metabolism of carbohydrates. Accordingly, we found that the canonical pathways *glycolysis I* and *gluconeogenesis I* were marked by the IPA analysis as highly influenced by BPA exposure. An extensive literature search was performed to complement the IPA analysis, and we identified more than 70 proteins influenced by BPA exposure, mostly upregulated, and related to carbohydrate and lipid metabolism and the generation of energy (Suppl. Table 1).

Glucose it is the major energy source for the ovary. However, the oocyte itself has a poor capacity to take up glucose, a limited apport of oxygen and a low glycolytic rate (Warzych and Lipinska, 2020a) Therefore, oocyte metabolism relies on cumulus cells (CCs) to convert

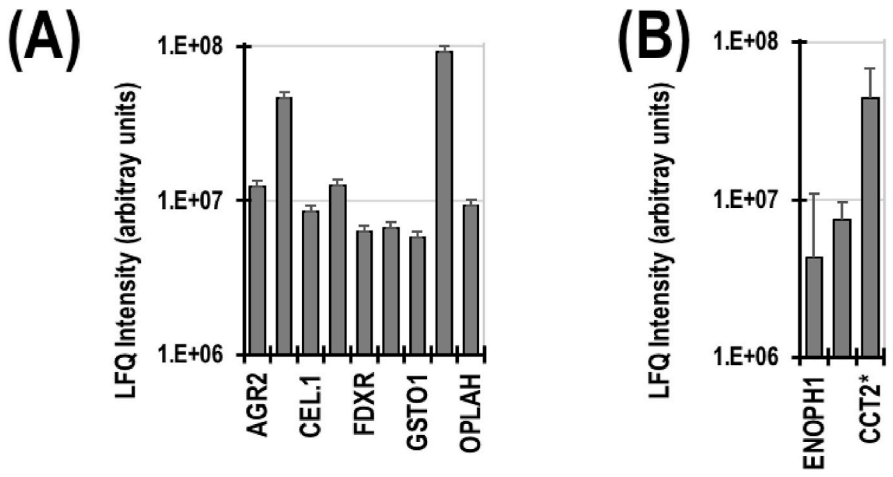

(C)

Protein names	*Abbreviation*	Fold change BPA/control
Alcohol dehydrogenase 8a	ADH8A	4.03
Alcohol dehydrogenase 8b	ADH8B	2.45
Aldehyde Dehydrogenase 8 Family Member A1	ALDH8A1	17.55
Aldo-keto reductase family 1 member A1-A	AKR1A1A	33.65
Aldo-keto reductase family 1, member B1 (aldose reductase)	AKR1B1.1	6.20
Catalase (EC 1.11.1.6)	CAT	2.99
NADPH:adrenodoxin oxidoreductase, mitochondrial	FDXR	8.46
Glutaredoxin (thioltransferase)	GLRX	2.23
Glutathione peroxidase 1	GPX1	5.37
Glutathione peroxidase 4	GPX4	2.68
Glutathione S-transferase, alpha tandem duplicate 1	GSTA4	7.72
Glutathione S-transferase mu tandem duplicate 2	GSTM2	8.82
Glutathione S-transferase omega 1	GSTO1	7.67
Glutathione S-transferase pi 1	GSTP1	4.52
Glutathione S-transferase rho	GSTR	3.47
Glutathione S-transferase theta 1a	GSTT1A	5.23
Glutathione S-transferase theta 1b	GSTT3	5.68
Glutathione S-transferase zeta 1	GSTZ1	9.03
Hemoglobin subunit alpha (Alpha-globin aa1)	HBAA1	5.80
Hemoglobin subunit beta-1 (Beta-1-globin)	HBBA1	6.37
Hemoglobin subunit beta-2 (Beta-2-globin)	HBBA2	5.35
Protein disulfide-isomerase	PDIA2	4.31
Superoxide dismutase [Cu-Zn]	SOD1	2.45
Thioredoxin	TXN	26.13

Fig. 5. Some proteins related to the canonical pathway NRF2-mediated Oxidative Stress Response affected by low-dose BPA (1 μg/L) exposure. Bars represent the log2 of averaged fluorescence intensity expressed in arbitrary units. **(A)** Proteins not detected **(ND)** in the control group; **(B)** proteins not detected in the BPA group; (**C**) fold-change variations of some representative proteins with increased abundance in the zebrafish ovary after BPA exposure.

glucose to pyruvate, lactate, malate and/or oxaloacetate. These metabolites enter the tricarboxylic pathway (TCA) to generate energy essential for oocyte development or are converted to glucose to be used in other metabolic pathways, such as glycolysis, the pentose phosphate pathway (PPP) and the hexosamine biosynthetic pathway (HBP) (Sutton-McDowall et al., 2010; Warzych and Lipinska, 2020a). Glucose catabolism during oocyte growth and maturation mostly occurs by aerobic glycolysis, which is independent of oxygen, as a means to protect mitochondria from Krebs cycle metabolism, which could lead to oxidative stress (Downs and Utecht, 1999; Warzych and Lipinska, 2020a). PPP utilizes a lower amount of glucose but generates NADPH and ribose-5-phosphate (R5P) for GSH, DNA and RNA synthesis (Sutton-McDowall et al., 2010). HBP converts glucose-6-phosphate (G6P) to UDP-N-acetyl glucosamine, which is mostly used to produce hyaluronic acid for matrix production. Only a minor part of UDP-N-acetyl glucosamine is used for O-linked glycosylation of proteins (Marshall et al., 1991), thus making HBP a cell-fuel sensor (Wells et al., 2003). Fig. 7 schematizes carbohydrate metabolism and some of the specific steps affected by BPA exposure and the fold-change variations in abundance of some of the proteins involved in the metabolism of carbohydrates, lipids and amino acids (see also Suppl. Table 1). Only a few enzymes were downregulated, but they determine the function of complete carbohydrate metabolism. The decreased levels of glycogenin 1 (GYG1, > 5-fold decrease) along with an increased concentration of amylo-alpha-1,6-glucosidase (AGLA, 9.8-fold increase) suggest that glycogen biosynthesis is inhibited and glucose-P units are liberated for

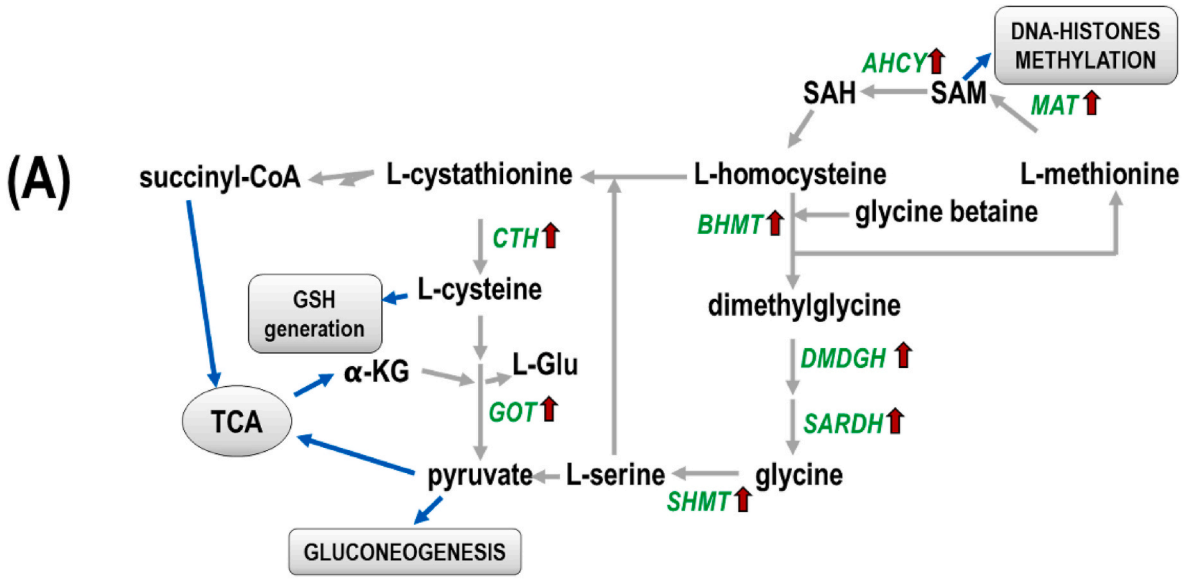

(B)

Protein names	*Abbreviation*	Fold change BPA/control
5-formyltetrahydrofolate cyclo-ligase	MTHFS	4.15
Adenosylhomocysteinase	AHCY	2.93
Aspartate aminotransferase (AST/GOT)	GOT1	5.31
Betaine--homocysteine S-methyltransferase 1	BHMT	6.77
Cystathionase (cystathionine gamma-lyase)	CTH	19.88
S-adenosylmethionine synthase	MAT1A	3.87
Sarcosine dehydrogenase	SARDH	3.84
Serine hydroxymethyltransferase 2	SHMT2	9.97

Fig. 6. (A) Integration of the glycine betaine degradation, methionine degradation and cysteine biosynthesis III pathways and their connection with oxidative stress and carbohydrate metabolism; the location of some ovarian proteins deregulated by low-dose BPA exposure are shown. Abbreviations: a-KG: a-ketoglutarate; L-Glu: L-glutamate; CTH: cystathionine gamma-lyase; AST: aspartate aminotransferase (glutamic-oxalacetic transaminase); BHMT: betaine-homocysteine S-methyltransferase; SHMT: serine hydroxymethyltransferase; DMDGH: dimethylglycine dehydrogenase; SARDH: sarcosine dehydrogenase; MAT: S-adenosylmethionine synthase; AHCY: adenosylhomocysteinase. **(B)** Fold-change variations in the abundance of proteins included in the one-carbon metabolism pathway.

use in other pathways. The HBP pathway was also negatively affected since UDP-N-acetylhexosamine pyrophosphorylase (UAP1L1) was not detected in the BPA group and increased the abundance of Glucosamine-6-phosphate isomerase (GNPDA), which drives the conversion of G6P into fructose 6-P (Fig. 7).

The amount of pyruvate kinase (PK) decreased 3.82-fold after BPA exposure. PK catalyzes the final step in glycolysis, converting phosphoenolpyruvate (PEP) and ADP to pyruvate and ATP. In most cells, the reaction is essentially irreversible and represents one of the major control points of glycolysis. PK inhibition acts as a switch between the glycolytic and gluconeogenic pathways. Hence, the observed inhibition of PK in the ovary of low-dose BPA-exposed zebrafish would increase the cellular concentration of glycolytic intermediates, enhancing gluconeogenesis and glucose breakdown via the PPP and accelerating the synthesis of NADPH and biomolecules such as pyrimidine and purine nucleotides in proliferating cells. Consistent with this finding, we also found that in BPA-exposed fish, high levels of glucose 6-phosphate dehydrogenase (G6PDH) were detected in the BPA ovarian fish. G6PDH is the first and rate-limiting enzyme of the PPP, and it is indispensable for maintaining the cytosolic pool of NADPH and thus the cellular redox balance and sustaining reductive biosynthetic processes. To fuel the PPP, several enzymes (phosphoglycerate mutase, PGM; glyceraldehyde-3-phosphate dehydrogenase, GAPDH; fructose-bisphosphate aldolase, ALDO; fructose-1,6-bisphosphatase, FBP) of the gluconeogenic pathway showed increased abundance, ranging from approx. 3- to 6-fold (Fig. 7; Suppl. Table 1), in the BPA-exposed zebrafish.

The metabolism and carbohydrates and lipids are closely related. Accordingly, we detected diminished levels of ATP-citrate lyase (ACLY, Suppl. Table 1, *Lipid metabolism, storing and transport* category) in the ovaries of low-dose BPA-exposed zebrafish. Cytosolic ACLY catalyzes the generation of acetyl-CoA from citrate escaped from the TCA, thereby linking glucose and/or glutamine metabolism and fatty acid synthesis and/or mevalonate pathways (Zaidi et al., 2012). Downregulation of ACLY drives the metabolites generated from pyruvate entering the mitochondria and those derived from different TCA anaplerotic reactions to gluconeogenesis. The increased levels of lactate dehydrogenase (LDH), isocitrate dehydrogenase (IDH), malate dehydrogenase (MDH) and malic enzyme (ME) act in conjunction with ACLY, thereby

(A)

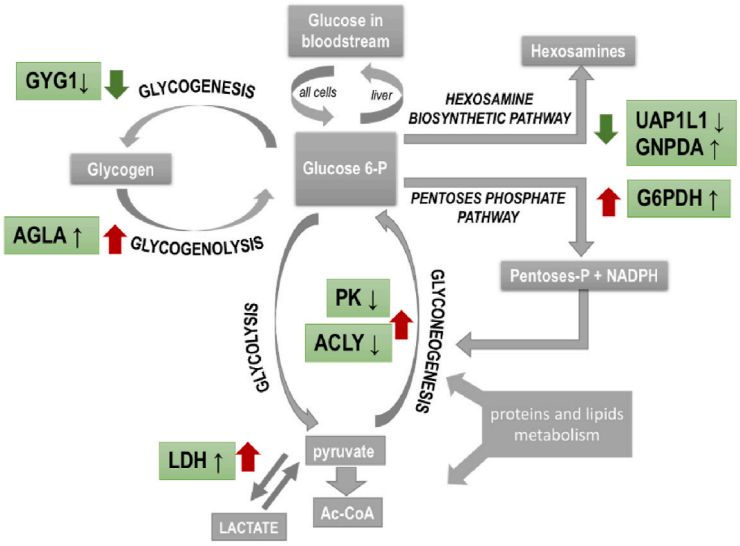

(B)

Protein names	Abbreviation	Fold change BPA/control
4-hydroxyphenylpyruvate dioxygenase	HPDA	5.32
Aconitase 1, soluble	ACO1	4.81
Adenylosuccinate synthetase	ADSSL	7.17
Aldose 1-epimerase	GALM	17.78
Amylo-alpha-1, 6-glucosidase-Enzima desramificadora del glucógeno	AGLA	9.77
ATP-citrate synthase	ACLYA	-2.36
Fructose-1,6-bisphosphatase 1b	FBP1B	3.49
Fructose-bisphosphate aldolase	ALDOAA	3.11
Fructose-bisphosphate aldolase B	ALDOB	6.21
Glucosamine-6-phosphate isomerase	GNPDA1	15.55
Glucose -6-phosphate dehydrogenase	G6PDH	20.69
Glutamate dehydrogenase 1	GLUD1B	3.97
Glyceraldehyde-3-phosphate dehydrogenase	GAPDH	3.15
Glycerol-3-phosphate dehydrogenase [NAD(+)]	GPD1C	2.95
Glycogenin 1	GYG1A	-5.23
Isocitrate dehydrogenase [NADP]	IDH1	5.93
L-lactate dehydrogenase A chain	LDHA	4.44
L-lactate dehydrogenase B-B chain	LDHBB	5.68
Malate dehydrogenase	MDH1AA	2.43
Malate synthase-like	MLSL	6.91
Malic enzyme	ME3	11.70
Malic enzyme (Fragment)	ME1	24.63
Phosphoenolpyruvate carboxykinase 2	PCK2	6.37
Phosphoglucomutase 5	PGM5	3.83
Phosphoglycerate mutase (EC 5.4.2.11)	PGAM1A	2.64
Pyruvate kinase	PK	-3.82
Succinyl-CoA synthetase subunit alpha	SUCLG1	2.04
UDP-glucose 6-dehydrogenase	UGDH	10.91
UDP-N-acetylhexosamine pyrophosphorylase-like protein 1	UAP1L1	-5.35
UTP--glucose-1-phosphate uridylyltransferase (EC 2.7.7.9)	UGP2A	2.84

Fig. 7. (A) Brief scheme of carbohydrate metabolism showing some of the routes affected by BPA exposure. (B) Fold-change variations in the abundance of some proteins related to carbohydrate metabolism pathway.

supplying pyruvate for gluconeogenesis and reducing energy, which counteracts the oxidative stress caused by BPA exposure (Sugiura et al., 2005; Sutton-McDowall et al., 2010; Xie et al., 2016).

In summary, our data suggest that low-dose BPA exposure leads to high glucose requirements in the ovary of zebrafish to almost exclusively fuel the PPP and produce NADPH and R5P, which are necessary for preserving the redox state through the reduction of glutathione to GSH and for the synthesis of large amounts of ribosomal RNA and heterogeneous RNA produced by nucleoli in the oocyte. NADPH/GSH would help to mitigate ROS generation, mitochondrial dysfunction, and BPA-induced changes in several signaling pathways related to oxidative stress, thereby helping to restore the antioxidant balance.

3.2.3. Low/dose BPA alters lipid metabolism, storing and transport and steroidogenesis

Lipid metabolism provides a potent source of energy during oocyte maturation (Olivares-Rubio and Vega-Lopez, 2016). During previtellogenic growth, lipids, mainly derived from circulating very low-density lipoprotein (VLDL) that binds to ovarian lipoprotein receptors, enter the oocyte. Endocytosed triacylglycerides (TAGs) are hydrolyzed into free fatty acids (FFAs) that are sequestered by cytoplasmic fatty acid binding proteins (FABP) to be finally used as a substrate for synthesis of

the neutral lipids stored in the ooplasm as lipid droplets, secreted to plasma or used to produce energy (Hiramatsu et al., 2015). In our proteomic analysis, seven FABP isoforms (FABP-1, -2, -3, -6, -7 -10 and −11) were detected in the ovaries of zebrafish (Suppl. Table 1 *Lipid metabolism, storing and transport* category), and the abundance of all isoforms increased (in the range of 2.7- to > 30-fold) after BPA exposure. It has been proposed that the different FABP ovarian subtypes play different roles in folliculogenesis, atresia, and hormone synthesis (Agulleiro et al., 2008). The observed increase in these specific FBPA subtypes might be associated with an increase in ovarian lipid deposition or secretion or altered use rates (Sant and Timme-Laragy, 2018). Few studies have addressed this issue. However, Fabp11 has been reported to be involved in the process of follicular atresia, and its 2.7-fold increase in abundance would contribute to the 3-fold increase in the percentage of atretic follicles reported in Fig. 3.

Glucose, pyruvate or lactate are essential for successful oocyte maturation, as discussed before. However, β-oxidation of FA (FAO) is an important energy source for oocyte development (Dunning et al., 2010; Warzych and Lipinska, 2020b). In the ovary of BPA-exposed zebrafish, reduced PK enzymes (Suppl. Table 1 *Carbohydrate metabolism and energy* category) lessen the generation of Ac-CoA from carbohydrates and strengthen the mitochondrial consumption of FAs, as deduced from the changes observed in several FAO proteins. FFAs from the extracellular milieu or intracellularly generated from lipid droplet stores first react in the cytoplasm with CoA catalyzed by acyl-CoA synthetase (ACFS). The acyl group is transferred to carnitine by carnitine O-acetyltransferase (CRAT) in a step prior to entering the mitochondrial matrix, where the successive actuation of ACFS, enoyl CoA hydratase (ECH), 3-hydroxy acyl-CoA dehydrogenase (SCHAD) and acetyl-CoA acyltransferase (ACAT) liberates Ac-CoA and a fatty acyl-CoA shortened by two carbon atoms. Low-dose BPA exposure increases the abundance of ACFS, CRAT and ACAT (Suppl. Table 1 *Lipid metabolism, storing and transport* category) and possibly the β-oxidation of FA in the ovary of zebrafish. It can be assumed that these changes occur to compensate for the energy lost by the deviation of glucose to non-ATP-producing pathways (as described above) and to generate the Ac-CoA needed in many metabolic pathways.

The reaction catalyzed by ACAT is reversible and used in the condensation of two Ac-CoA molecules into acetoacetyl-CoA to initiate the synthesis of cholesterol and steroid hormones. Cholesterol is a fundamental lipid in cells and responsible for the proper organization and function of membranes and the precursor of all steroid hormones. However, most cholesterol utilized for steroid synthesis is derived from the cellular uptake of low-density lipoproteins (LDL) by receptor-mediated endocytosis. Lipoprotein-free cholesterol is then managed by proteins (Niemann-Pick type proteins, Annexins, and small Rab GTPases) that drive it to different organelles through sophisticated circuits to regulate its intracellular sorting, trafficking and storage to avoid free cholesterol cytotoxicity (Meneses-Salas et al., 2020). Related to cholesterol, and associated to low-dose BPA exposure, we observed important increases in the abundance of seven Annexin isoenzymes (ANXA1a, 2a, 2b, 3b, 5b, 11b, 13) in the zebrafish ovary, some of which were undetected in the control samples, and two Rab proteins (RAB2a, 10) (Suppl. Table 1 *Lipid metabolism, storing and transport* category). Soluble Ca^{2+}-regulated Annexin and Rab (RAS genes from rat brain)-GTPases are implicated in both endocytosis and exocytosis and hence in intracellular cholesterol trafficking and metabolism (Enrich et al., 2011; Veleri et al., 2018). Overexpression of AnxA has been associated with cholesterol accumulation in late endosomes and reduced cholesterol levels at the plasma membrane (increased permeability to small molecules, alterations in cell-to cell relationships), mitochondria (reduced steroidogenesis) and Golgi apparatus (reduced exocytic route) (Meneses-Salas et al., 2020). Another protein, ApoA-IV (Suppl. Table 1 *Lipid metabolism, storing and transport* category), which is associated with chilomicrones and HDL in plasma and involved in free cholesterol efflux (i.e., 'reverse cholesterol transport'), was present in the ovary of the control group but was not detected after BPA exposure (Suppl. Table 1). ApoA-IV is a clear link between lipid and carbohydrate metabolism, as it also regulates glucose homeostasis and its deficiency would contribute to cholesterol retention but would also improve gluconeogenesis and decrease de novo lipogenesis in the liver (Wang et al., 2019), as previously discussed.

Steroidogenesis starts with the transport of cholesterol to the inner mitochondrial membrane mediated by steroidogenic acute regulatory protein (StAR) (Devoto et al., 2002). Cytochrome P450-side-chain-cleavage (SCC, CYP11A1)/ferredoxin reductase (FDXR) metabolon (Midzak and Papadopoulos, 2016) converts cholesterol into pregnenolone (P5). P5 diffuses into the smooth endoplasmic space, where different cytochromes catalyze their conversion into androstenedione and testosterone, finally transformed by ovarian aromatase CYP19A1 into estrogen and estradiol, respectively. StAR is a member of the steroidogenic transduceosome, a multiprotein complex traversing the outer and internal membranes of steroidogenic mitochondria that controls cholesterol trafficking and targeting into mitochondria (Rone et al., 2012). StAR is negatively regulated by 14-3-3 proteins, members of the transduceosome/metabolon complex and regulators of steroidogenesis (Tugaeva et al., 2020). The observed abundance increases in the zebrafish ovary of two 14-3-3 protein isoforms after BPA exposure (Suppl. Table 1 *Lipid metabolism, storing and transport* category) would reduce the functionality of StAR, arresting the synthesis of steroids and leading to the accumulation of cholesterol-enriched lipid droplets in the cytoplasm of steroidogenic cells (Miller and Bose, 2011). However, we also observed increased levels of sterol carrier protein 2 (SCP2, Suppl. Table 1 *Lipid metabolism, storing and transport* category) in the BPA-exposed ovary. SCP2 participates in the movement of cholesterol between vesicles and mitochondria and has been reported to stimulate mitochondrial pregnenolone synthesis (Li et al., 2016). Multiple studies have investigated the association between BPA exposure and ovarian steroidogenesis in women, rodents and cells. BPA has been proven to disrupt gonadal steroidogenesis in mammals and fish (Bloom et al., 2016; Mahalingam et al., 2017; Molina et al., 2018b), but the results are equivocal and indicate different consequences over estradiol, testosterone, Cyp19 (aromatase), and Star (steroidogenic acute regulatory protein) (Mlynarcikova et al., 2014; Peretz et al., 2014). Our data suggest that low-dose BPA exposure alters membrane functionality, cholesterol trafficking and cholesterol export and compromises some crucial steps in steroid synthesis. The impact of BPA on StAR abundance and activity and, consequently, on the amount of mitochondrial cholesterol disponible for steroidogenesis are unknown. However, a recent study in *Caenorhabditis elegans* demonstrated that BPA exposure impairs the StAR-mediated transport of cholesterol into the mitochondria and alters intracellular cholesterol distribution (Chen et al., 2019), thus supporting our results. In addition, it has been reported that exposure to 1 μg/L BPA reduces the transcript counts of the StAR gene (Biswas et al., 2020). From these results, we hypothesized that exposure to low concentrations of BPA disrupts 17β-estradiol production via the alteration of steroidogenic protein abundance and cholesterol homeostasis in zebrafish ovarian cells.

BPA may also affect the steroidogenic capacity of the ovary via induction of peroxisome proliferator–activated receptor-γ (PPARγ), thereby causing a decrease in the expression of aromatase (Cyp19a1) and consequently leading to diminished estradiol production (Kwintkiewicz et al., 2010). In a previous work, we demonstrated that 1 μg/L BPA impairs the synthesis of steroids through the inhibition, at the transcriptional level, of the ovarian aromatase CYP19A1, the enzyme that converts androstenedione to estrone and testosterone to 17β-estradiol (Molina et al., 2018b). In the present proteomic study, we did not detect the aromatase protein, even in the control samples, which was probably because the changes caused at the protein level were not statistically significant under the stringent conditions of our proteomic analysis. However, the dysregulation of some proteins linked to retinoid metabolism suggests that in the BPA-exposed zebrafish ovary, PPAR

induction occurred. PPARs are a group of nuclear receptors that bind DNA as heterodimers with retinoid receptors (RXRs) on PPAR response elements (PPREs) to control a variety of genes involved in several pathways of lipid and glucose metabolism (Olsen and Blomhoff, 2020). Members of the PPAR family also participate in primordial follicle activation and development (Yoon et al., 2020). Recently, many groups have identified new connections between retinoid metabolism and PPAR responses. Retinoids are vitamin A derivatives that coordinate energy balance by activating specific nuclear receptors, such as RXR or PPARs. These metabolites have been reported to be involved in cell differentiation, cell cycle differentiation, cell cycle control, cell growth, and cellular responses to cell injury as well as in obesity, diabetes, and cardiovascular diseases (Olsen and Blomhoff, 2020). In addition, retinoid homeostasis is essential to providing molecular control of follicular development, steroidogenesis and oocyte maturation in the ovary (Jiang et al., 2017a). Retionid acid (RA), the vitamin A active form, is synthetized from retinol by the successive actuation of alcohol dehydrogenase (ADH), which transforms retinol to retinal, and acetaldehyde dehydrogenase (ALDH), which oxidizes retinal to RA. RA levels are controlled by the actuation RA regulates transcription by binding to RA receptors (RARs) or RXRs. These proteins combine with other partners (such as PPARs) to serve as DNA sequence-specific transcription factors. RA levels are controlled by the actuation of Aldo-keto reductases (AKR), which oxidize retinal back to retinol, and retinol saturase (RetSat), which saturates the 13–14 double bond of retinol to produce (via RAR) dehydroretinol, a potent inductor of the RA-degrading enzyme cytochrome P450 26a1 (Cyp26a1). The same enzymes acting on retinol transform dehydroretinol into dehydroretinoic acid, which is unable to activate transcription through RXR (Moise et al., 2007). In the ovaries of low-dose BPA-exposed zebrafish, we found a pronounced decrease in the abundance of RetSat (approximately 30-fold, Suppl. Table 1 *Cell signaling* category) and notable increases in the levels of AKR enzymes (up > 30-fold, Suppl. Table 1 *NRF2 and related antioxidative proteins* category). This result suggested a possible reduction in retinal and the RA signaling pathways after BPA exposure. Since abnormal retinoid signaling is involved in ovarian physiology and pathogenesis of polycystic ovary syndrome in mammals (Jiang et al., 2017b) and zebrafish (Rodríguez-Marí et al., 2013), it is evident that the reduction of the RA pathway would deprive the ovary of important regulators of oogenesis maturation and oocyte survival.

3.2.4. *Low/dose BPA forces stage I follicle progression throughout previtellogenic and vitellogenic phases*

Perhaps the most striking result obtained in this work was the large effect of BPA exposure on the abundance of vitellogenins (VTGs), with zebrafish exposure to 1 μg/L BPA leading to a reduction of the different VTG isoforms to less than 4.2–11.2 % (Fig. 8, Suppl. Table 1 *Lipid metabolism, storing and transport* category); in contrast, only a small reduction in the number of vitellogenic follicles can be seen in Fig. 3.

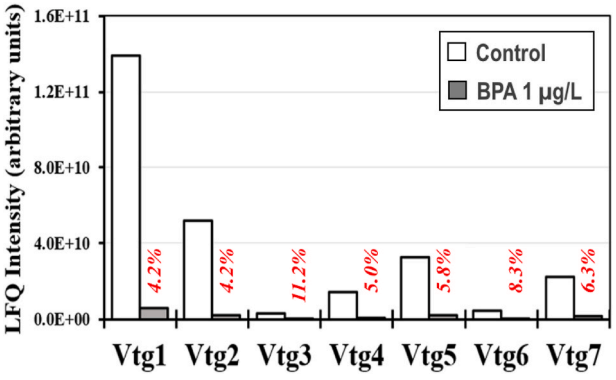

Fig. 8. Abundance of VTG protein isoforms in the control and the **low-dose BPA (1 μg/L) zebrafish ovaries.** Numbers over the dark bars represent the percentage of each VTG isoform in the BPA samples regarding to that found in the control.

VTGs are large, very high-density glycolipoproteins exclusively synthesized during oogenesis, mainly in the liver of most non-mammalian species, including zebrafish, and transported through the blood to developing follicles. VTGs enter the oocyte through receptor-mediated endocytosis during the late previtellogenic and early vitellogenic stages. In oocytes, VTG is cleaved by cathepsin into smaller yolk proteins (phosvitin, lipovitellin proteins, and smaller β′ components) used as nutrients for embryonic development (Hiramatsu et al., 2015). Zebrafish have eight different VTGs encoded by different genes. VTG1, 4, 5, 6 and 7 are the major contributors to developmental and nutritional processes in both embryos and larvae (Yilmaz et al., 2019). In teleosts, 17β–estradiol binds to the hepatic estrogen receptor (ER) to activate the synthesis of VTG in the liver. Accordingly, an increase in the total levels of VTG is expected, as we showed in a previous paper (Molina et al., 2018b). In that paper, we also showed that 1 μg/L BPA exposure depleted the production of aromatase in the ovary, impairing the ovarian production of estradiol and, therefore, that of VTG. The reduced levels of VTG in the ovary of 1 μg/L BPA-exposed zebrafish that we observed here (Fig. 8, Suppl. Table 1 *Lipid metabolism, storing and transport* category) cannot be explained only by low internal production but might be attributed to an effect of BPA on the mechanisms of incorporation of VTG into the ovary. We discussed above that low-dose BPA exposure altered membrane functionality. From the data presented here, it could also be inferred that the VTG import resulted compromised after BPA exposure, which would affect zebrafish fertility. Future studies will discern whether BPA impairs the plasma membrane Vtg-receptor (VtgR) system by specific binding that avoids VTG binding and ovary incorporation.

However, other explanations cannot be ruled out. By using slightly higher BPA doses (5 μg/L), Migliaccio et al. (2018b) suggested that BPA promotes a potential model of follicle atresia peculiarly responsive to BPA, in which BPA promotes the atretic development of early recruited stage I follicles by accelerating and forcing their progression throughout previtellogenic and vitellogenic phases. This premature development of stage II follicles slows down their vitellogenic entry with prematurely formed yolk granules, where vitellogenins are proteolytic processes. Proteolysis has been shown to underlie the oocyte hydration event occurring in all teleosts to provide the single-celled egg with an essential pool of water for survival during early development in the saline oceanic environment (Kristoffersen et al., 2009). Similarly, it has been reported that oxidative stress has the ability to induce zebrafish oocyte maturation by inducing apoptosis in ovarian follicle cells (Chen et al., 2017). In support of this hypothesis, we found increased levels of proteins globally enclosed in the degradome (including the SPINK1 Pancreatic Cancer Pathway identified in the IPA® analysis), such as cathepsins or serine proteases, involved in the process of yolk formation during oocyte maturation, having a fundamental role in fish reproductive success (Carnevali and Maradonna, 2003). Similar results have been described in human neutrophils exposed to BPA (Ratajczak-Wrona et al., 2019). However, we also found increased levels of protease inhibitors, such as serpins, suggesting that the cell attempts to counteract the effects of this acute low dose of BPA exposure.

3.2.5. *Ovarian ubiquitin/proteasome (degradome) pathway results affected by low/dose BPA exposure*

Increased abundance of several ubiquitination-related proteins and a strong diminution of proteasome components were observed in the ovaries of zebrafish exposed to 1 μg/L BPA (Suppl. Table 1, *Degradome* pathway). The ubiquitin-proteasome pathway (UPP) is the major extralysosomal pathway responsible for intracellular protein degradation in eukaryotes and a central player in the regulation of several diverse cellular processes. UPP targets specific proteins for destruction through an enzymatic process that marks the proteins that must be

degraded by covalent bonding of a polyubiquitin chain. Proteasomal degradation is necessary for the completion of the first meiotic division (Dekel, 2005). Our data suggest that the proteasome is a potential target of nanomolar BPA toxicity in zebrafish ovaries (Suppl. Table 1, *Degradome* pathway). Although described at the transcriptional level (Ge et al., 2014), to our knowledge, this is the first report revealing the downregulation of proteasomal proteins by nanomolar BPA exposure. The upregulation of ubiquitin activity along with the downregulation of the proteasome by nanomolar BPA could lead to the accumulation of ubiquitinated proteins. Consequently, cell proliferation is inhibited, apoptosis is activated (Gupta et al., 2018) and atresia occurs. Evidence suggests that other proteolytic pathways can partially compensate for intracellular polyubiquitinated protein degradation when UPS activity is insufficient (Liebl and Hoppe, 2016), explaining the low level of atresia observed in the ovaries of zebrafish exposed to 1 μg/L BPA.

4. Conclusions

Our data showed that low-dose (1 μg/L) BPA exposure for a short time (14 days) caused ROS generation, although ovarian cells were able to avoid large-scale tissue damage by inducing the NRF2-mediated oxidative stress response, auxiliary proteins, such as hemoglobin, and many other proteins that led to the abundance of GSH by enhanced cysteine, glutamic acid and glycine generation pathways through one-carbon metabolism alterations, which may also change the DNA methylation pattern. Increased gluconeogenesis produces glucose to fuel the PPP and produce NADPH, thereby helping to restore the antioxidant balance. BPA also alters steroidogenic protein abundance and cholesterol homeostasis in zebrafish ovarian cells, probably via induction of peroxisome PPARγ and a severe reduction in retinal and RA signaling pathways, thus depriving the ovary of important regulators of oogenesis maturation and oocyte survival. Our proteomic results also indicate that low-dose BPA exposure alters the proteolytic pathways in ovarian cells, accelerates follicle maturation and induces atresia.

Overall, the data presented in this study suggest that nanomolar BPA exposure causes strong alterations at the molecular level that have potential negative effects on reproduction. Although these alterations are not reflected at the histological level because of the short experimental time, we postulated that BPA pollutant concentrations should be controlled at below-nanomolar levels because inadvertent exposure to small concentrations of BPA on a continuous basis may influence the quality of the oocyte and increase the occurrence of ovarian cancer in the long term through deregulation of DNA methylation patterns, metabolism and proteostasis.

Author contributions

Ana M[a] Molina: conceptualization, data curation, formal analysis, investigation, methodology, validation, visualization; writing original draft ± review & editing; ***Nieves Abril:*** conceptualization, resources, proteomic analysis, data curation, formal analysis, investigation, methodology, validation, supervision, writing original draft ± review & editing; ***Antonio J. Lora:*** investigation, methodology, writing ± review & editing; ***Paula V Huertas-Abril:*** proteomic analysis, investigation, writing ± review; ***Nahum Ayala:*** investigation, methodology, writing ± review & editing; ***Carmen Blanco:*** histological investigation, methodology, writing ± review & editing ***M[a] Rosario Moyano:*** conceptualization, investigation, funding acquisition, project administration, resources, supervision, visualization, writing ± review & editing.

Declaration of competing interest

The authors declare that they have no known competing financial interests or personal relationships that could have appeared to influence the work reported in this paper.

Acknowledgments

This work was supported by Spanish Junta de Andalucía (grant P09-AGR-5143).

The authors would like to thank the PAB (Plataforma Andaluza de Bioinformática- SCBI Universidad de Málaga) for its use during this research.

We thank Noelia Morales-Prieto, University College Cork (UCC), Cork, Ireland, for her assistant during the preparation of samples. Carlos A. Fuentes-Almagro, from the Genomic Service from the Central Services for Research of the University of Córdoba (SCAI) for his support with the proteomic analysis, and all the Experimental Animal Service staff for their support during the experimental procedure.

Appendix A. Supplementary data

Supplementary data to this article can be found online at https://doi.org/10.1016/j.fct.2021.112435.

References

Agulleiro, M.J., Andre, M., Morais, S., Cerda, J., Babin, P.J., 2008. High transcript level of a fatty acid-binding protein 11 but not of vitellogenin receptor is correlated to ovarian follicle atresia in a teleost fish (Solea senegalensis). Cybium 32, 225-225.
Andra, S.S., Austin, C., Yang, J., Patel, D., Arora, M., 2016. Recent advances in simultaneous analysis of bisphenol A and its conjugates in human matrices: exposure biomarker perspectives. Sci. Total Environ. 572, 770–781.
Badding, M.A., Barraj, L., Williams, A.L., Scrafford, C., Reiss, R., 2019. CLARITY-BPA Core Study: analysis for non-monotonic dose-responses and biological relevance. Food Chem. Toxicol. 131, 110554.
Benjamini, Y., Hochberg, Y., 1995. Controlling the false discovery rate: a practical and powerful approach to multiple testing. J. Roy. Stat. Soc. B 57, 289–300.
Berger, A., Ziv-Gal, A., Cudiamat, J., Wang, W., Zhou, C., Flaws, J.A., 2016. The effects of in utero bisphenol A exposure on the ovaries in multiple generations of mice. Reprod. Toxicol. 60, 39–52.
Biswas, S., Ghosh, S., Samanta, A., Das, S., Mukherjee, U., Maitra, S., 2020. Bisphenol A impairs reproductive fitness in zebrafish ovary: potential involvement of oxidative/nitrosative stress, inflammatory and apoptotic mediators. Environ. Pollut. 267, 115692.
Bloom, M.S., Mok-Lin, E., Fujimoto, V.Y., 2016. Bisphenol A and ovarian steroidogenesis. Fertil. Steril. 106, 857–863.
Bradford, M.M., 1976. A rapid and sensitive method for the quantitation of microgram quantities of protein utilizing the principle of protein-dye binding. Anal. Biochem. 72, 248–254.
Calafat, A.M., Ye, X., Wong, L.Y., Reidy, J.A., Needham, L.L., 2008. Exposure of the U.S. population to bisphenol A and 4-tertiary-octylphenol: 2003-2004. Environ. Health Perspect. 116, 39–44.
Carnevali, O., Maradonna, F., 2003. Exposure to xenobiotic compounds: looking for new biomarkers. Gen. Comp. Endocrinol. 131, 203–208.
Chen, S.X., Yang, X.Z., Deng, Y., Huang, J., Li, Y., Sun, Q., Yu, C.-P., Zhu, Y., Hong, W.S., 2017. Silver nanoparticles induce oocyte maturation in zebrafish (Danio rerio). Chemosphere 170, 51–60.
Chen, Y., Panter, B., Hussain, A., Gibbs, K., Ferreira, D., Allard, P., 2019. BPA interferes with StAR-mediated mitochondrial cholesterol transport to induce germline dysfunctions. Reprod. Toxicol. 90, 24–32.
Chepelev, N.L., Enikanolaiye, M.I., Chepelev, L.L., Almohaisen, A., Chen, Q., Scoggan, K. A., Coughlan, M.C., Cao, X.L., Jin, X., Willmore, W.G., 2013. Bisphenol A activates the Nrf1/2-antioxidant response element pathway in HEK 293 cells. Chem. Res. Toxicol. 26, 498–506.
Cox, J., Hein, M.Y., Luber, C.A., Paron, I., Nagaraj, N., Mann, M., 2014. Accurate proteome-wide label-free quantification by delayed normalization and maximal peptide ratio extraction, termed MaxLFQ. Mol. Cell. Proteomics 13, 2513–2526.
Dekel, N., 2005. Cellular, biochemical and molecular mechanisms regulating oocyte maturation. Mol. Cell. Endocrinol. 234, 19–25.
Devoto, L., Kohen, P., Vega, M., Castro, O., González, R.R., Retamales, I., Carvallo, P., Christenson, L.K., Strauss, J.F., 2002. Control of human luteal steroidogenesis. Mol. Cell. Endocrinol. 186, 137–141.
Downs, S.M., Utecht, A.M., 1999. Metabolism of radiolabeled glucose by mouse oocytes and oocyte-cumulus cell complexes. Biol. Reprod. 60, 1446–1452.
Dunning, K.R., Cashman, K., Russell, D.L., Thompson, J.G., Norman, R.J., Robker, R.L., 2010. Beta-oxidation is essential for mouse oocyte developmental competence and early embryo development. Biol. Reprod. 83, 909–918.
Efsa, 2015. https://efsa.onlinelibrary.wiley.com/doi/epdf/10.2903/j.efsa.2015.3978.
Enrich, C., Rentero, C., de Muga, S.V., Reverter, M., Mulay, V., Wood, P., Koese, M., Grewal, T., 2011. Annexin A6-Linking Ca2+ signaling with cholesterol transport. Bba-Mol Cell Res 1813, 935–947.
Gassman, N.R., 2017. Induction of oxidative stress by bisphenol A and its pleiotropic effects. Environ. Mol. Mutagen. 58, 60–71.
Ge, L.C., Chen, Z.J., Liu, H., Zhang, K.S., Su, Q., Ma, X.Y., Huang, H.B., Zhao, Z.D., Wang, Y.Y., Giesy, J.P., Du, J., Wang, H.S., 2014. Signaling related with biphasic

effects of bisphenol A (BPA) on Sertoli cell proliferation: a comparative proteomic analysis. Biochim. Biophys. Acta 1840, 2663–2673.
González-Kother, P., Oliva, M.E., Tanguy, A., Moraga, D., 2020. A review of the potential genes implicated in follicular atresia in teleost fish. Marine Genomics 50, 100704.
Guo, J., Zhao, M.-H., Shin, K.-T., Niu, Y.-J., Ahn, Y.-D., Kim, N.-H., Cui, X.-S., 2017. The possible molecular mechanisms of bisphenol A action on porcine early embryonic development. Sci. Rep. 7, 8632.
Gupta, I., Singh, K., Varshney, N.K., Khan, S., 2018. Delineating crosstalk mechanisms of the ubiquitin proteasome system that regulate apoptosis. Frontiers in Cell and Developmental Biology 6, 11.
Hiramatsu, N., Todo, T., Sullivan, C.V., Schilling, J., Reading, B.J., Matsubara, T., Ryu, Y. W., Mizuta, H., Luo, W.S., Nishimiya, O., Wu, M.Q., Mushirobira, Y., Yilmaz, O., Hara, A., 2015. Ovarian yolk formation in fishes: molecular mechanisms underlying formation of lipid droplets and vitellogenin-derived yolk proteins. Gen. Comp. Endocrinol. 221, 9–15.
Hui, L., Li, H., Lu, G., Chen, Z., Sun, W., Shi, Y., Fu, Z., Huang, B., Zhu, X., Lu, W., Xia, D., Wu, Y., 2018. Low dose of bisphenol A modulates ovarian cancer gene expression profile and promotes epithelial to mesenchymal transition via canonical wnt pathway. Toxicol. Sci. : an official journal of the Society of Toxicology 164 (2), 527–538, 2018.
Jia, L., Li, J., He, B., Jia, Y., Niu, Y., Wang, C., Zhao, R., 2016. Abnormally activated one-carbon metabolic pathway is associated with mtDNA hypermethylation and mitochondrial malfunction in the oocytes of polycystic gilt ovaries. Sci. Rep. 6, 19436-19436.
Jiang, Y., Li, C., Chen, L., Wang, F., Zhou, X., 2017a. Potential role of retinoids in ovarian physiology and pathogenesis of polycystic ovary syndrome. Clin. Chim. Acta 469, 87–93.
Jiang, Y., Li, C., Chen, L., Wang, F., Zhou, X., 2017b. Potential role of retinoids in ovarian physiology and pathogenesis of polycystic ovary syndrome. Clinica chimica acta; international journal of clinical chemistry 469, 87–93.
Kristoffersen, B.A., Nerland, A., Nilsen, F., Kolarevic, J., Finn, R.N., 2009. Genomic and proteomic analyses reveal non-neofunctionalized vitellogenins in a basal clupeocephalan, the Atlantic herring, and point to the origin of maturational yolk proteolysis in marine teleosts. Mol. Biol. Evol. 26, 1029–1044.
Kwintkiewicz, J., Nishi, Y., Yanase, T., Giudice, L.C., 2010. Peroxisome proliferator-activated receptor-gamma mediates bisphenol A inhibition of FSH-stimulated IGF-1, aromatase, and estradiol in human granulosa cells. Environ. Health Perspect. 118, 400–406.
Lee, M.B., Kooistra, M., Zhang, B., Slow, S., Fortier, A.L., Garrow, T.A., Lever, M., Trasler, J.M., Baltz, J.M., 2012. Betaine homocysteine methyltransferase is active in the mouse blastocyst and promotes inner cell mass development. J. Biol. Chem. 287, 33094–33103.
Li, D., Liu, H.X., Fang, Y.Y., Huo, J.N., Wu, Q.J., Wang, T.R., Zhou, Y.M., Wang, X.X., Ma, X.X., 2018. Hyperhomocysteinemia in polycystic ovary syndrome: decreased betaine-homocysteine methyltransferase and cystathionine β-synthase-mediated homocysteine metabolism. Reprod. Biomed. Online 37, 234–241.
Li, J., Ge, W., 2020. Zebrafish as a model for studying ovarian development: recent advances from targeted gene knockout studies. Mol. Cell. Endocrinol. 507, 110778.
Li, N.C., Fan, J., Papadopoulos, V., 2016. Sterol carrier protein-2, a nonspecific lipid-transfer protein, in intracellular cholesterol trafficking in testicular leydig cells. PloS One 11, e0149728.
Li, S., Sun, Q., Wu, Q., Gui, W., Zhu, G., Schlenk, D., 2019. Endocrine disrupting effects of tebuconazole on different life stages of zebrafish (Danio rerio). Environ. Pollut. 249, 1049–1059.
Liebl, M.P., Hoppe, T., 2016. It's all about talking: two-way communication between proteasomal and lysosomal degradation pathways via ubiquitin. Am. J. Physiol. Cell Physiol. 311, C166–C178.
Lim, M., Brown, H.M., Kind, K.L., Thompson, J.G., Dunning, K.R., 2019. Hemoglobin: potential roles in the oocyte and early embryo†. Biol. Reprod. 101, 262–270.
Lindholst, C., Wynne, P.M., Marriott, P., Pedersen, S.N., Bjerregaard, P., 2003. Metabolism of bisphenol A in zebrafish (Danio rerio) and rainbow trout (Oncorhynchus mykiss) in relation to estrogenic response. Comp. Biochem. Physiol. C Toxicol. Pharmacol. 135 (2), 169–177.
Lubzens, E., Young, G., Bobe, J., Cerdà, J., 2010. Oogenesis in teleosts: how fish eggs are formed. Gen. Comp. Endocrinol. 165, 367–389.
Mahalingam, S., Ther, L., Gao, L., Wang, W., Ziv-Gal, A., Flaws, J.A., 2017. The effects of in utero bisphenol A exposure on ovarian follicle numbers and steroidogenesis in the F1 and F2 generations of mice. Reprod. Toxicol. 74, 150–157.
Maleedhu, P., M, V., S, S.B.S., Kodumuri, P.K., Devi, D.V., 2014. Status of homocysteine in polycystic ovary syndrome (PCOS). J. Clin. Diagn. Res. : J. Clin. Diagn. Res. 8, 31–33.
Marshall, S., Bacote, V., Traxinger, R.R., 1991. Complete inhibition of glucose-induced desensitization of the glucose transport system by inhibitors of mRNA synthesis. Evidence for rapid turnover of glutamine:fructose-6-phosphate amidotransferase. J. Biol. Chem. 266, 10155–10161.
Martín, J., Santos, J.L., Aparicio, I., Alonso, E., 2019. Exposure assessment to parabens, bisphenol A and perfluoroalkyl compounds in children, women and men by hair analysis. Sci. Total Environ. 695, 133864.
Matuszczak, E., Komarowska, M.D., Debek, W., Hermanowicz, A., 2019. The impact of bisphenol A on fertility, reproductive system, and development: a review of the literature. International journal of endocrinology 4068717, 2019.
Meli, R., Monnolo, A., Annunziata, C., Pirozzi, C., Ferrante, M.C., 2020. Oxidative stress and BPA toxicity: an antioxidant approach for male and female reproductive dysfunction. Antioxidants 9, 405.
Meneses-Salas, E., García-Melero, A., Kanerva, K., Blanco-Muñoz, P., Morales-Paytuvi, F., Bonjoch, J., Casas, J., Egert, A., Beevi, S.S., Jose, J., Llorente-Cortés, V., Rye, K.-A., Heeren, J., Lu, A., Pol, A., Tebar, F., Ikonen, E., Grewal, T., Enrich, C., Rentero, C., 2020. Annexin A6 modulates TBC1D15/Rab7/StARD3 axis to control endosomal cholesterol export in NPC1 cells. Cell. Mol. Life Sci. 77, 2839–2857.
Midzak, A., Papadopoulos, V., 2016. Adrenal mitochondria and steroidogenesis: from individual proteins to functional protein assemblies. Front. Endocrinol. 7.
Migliaccio, M., Chioccarelli, T., Ambrosino, C., Suglia, A., Manfrevola, F., Carnevali, O., Fasano, S., Pierantoni, R., Cobellis, G., 2018a. Characterization of follicular atresia responsive to BPA in zebrafish by morphometric analysis of follicular stage progression. International journal of endocrinology 4298195, 2018.
Migliaccio, M., Chioccarelli, T., Ambrosino, C., Suglia, A., Manfrevola, F., Carnevali, O., Fasano, S., Pierantoni, R., Cobellis, G., 2018b. Characterization of follicular atresia responsive to BPA in zebrafish by morphometric analysis of follicular stage progression. International journal of endocrinology 4298195, 2018.
Miller, W.L., Bose, H.S., 2011. Early steps in steroidogenesis: intracellular cholesterol trafficking. J. Lipid Res. 52, 2111–2135.
Mlynarcikova, A., Fickova, M., Scsukova, S., 2014. Impact of endocrine disruptors on ovarian steroidogenesis. Endocr. Regul. 48, 201–224.
Moise, A.R., Isken, A., Domínguez, M., de Lera, A.R., von Lintig, J., Palczewski, K., 2007. Specificity of zebrafish retinol saturase: formation of all-trans-13,14-dihydroretinol and all-trans-7,8- dihydroretinol. Biochemistry 46, 1811–1820.
Molina, A., Abril, N., Morales-Prieto, N., Monterde, J., Ayala, N., Lora, A., Moyano, R., 2018a. Hypothalamic-pituitary-ovarian axis perturbation in the basis of bisphenol A (BPA) reproductive toxicity in female zebrafish (Danio rerio). Ecotoxicol. Environ. Saf. 156, 116–124.
Molina, A.M., Abril, N., Morales-Prieto, N., Monterde, J.G., Lora, A.J., Ayala, N., Moyano, R., 2018b. Evaluation of toxicological endpoints in female zebrafish after bisphenol A exposure. Food Chem. Toxicol. 112, 19–25.
Molina, A.M., Lora, A.J., Blanco, A., Monterde, J.G., Ayala, N., Moyano, R., 2013. Endocrine-active compound evaluation: qualitative and quantitative histomorphological assessment of zebrafish gonads after bisphenol-A exposure. Ecotoxicol. Environ. Saf. 88, 155–162.
Murata, M., Kang, J.-H., 2018. Bisphenol A (BPA) and cell signaling pathways. Biotechnol. Adv. 36, 311–327.
Newman, A.C., Maddocks, O.D.K., 2017. One-carbon metabolism in cancer. Br. J. Canc. 116, 1499–1504.
Nunes, S.C., Ramos, C., Lopes-Coelho, F., Sequeira, C.O., Silva, F., Gouveia-Fernandes, S., Rodrigues, A., Guimarães, A., Silveira, M., Abreu, S., Santo, V.E., Brito, C., Félix, A., Pereira, S.A., Serpa, J., 2018. Cysteine allows ovarian cancer cells to adapt to hypoxia and to escape from carboplatin cytotoxicity. Sci. Rep. 8, 9513.
Olivares-Rubio, H.F., Vega-Lopez, A., 2016. Fatty acid metabolism in fish species as a biomarker for environmental monitoring. Environ. Pollut. 218, 297–312.
Olsen, T., Blomhoff, R., 2020. Retinol, retinoic acid, and retinol-binding protein 4 are differentially associated with cardiovascular disease, type 2 diabetes, and obesity: an overview of human studies. Advances in nutrition (Bethesda, Md.) 11, 644–666.
Patiño, R., Sullivan, C.V., 2002. Ovarian follicle growth, maturation, and ovulation in teleost fish. Fish Physiol. Biochem. 26, 57–70.
Patel, S., Brehm, E., Gao, L., Rattan, S., Ziv-Gal, A., Flaws, J.A., 2017. Bisphenol A exposure, ovarian follicle numbers, and female sex steroid hormone levels: results from a CLARITY-BPA study. Endocrinology 158 (6), 1727–1738.
Peretz, J., Vrooman, L., Ricke, W.A., Hunt, P.A., Ehrlich, S., Hauser, R., Padmanabhan, V., Taylor, H.S., Swan, S.H., VandeVoort, C.A., Flaws, J.A., 2014. Bisphenol a and reproductive health: update of experimental and human evidence, 2007-2013. Environ. Health Perspect. 122, 775–786.
Prins, G.S., Patisaul, H.B., Belcher, S.M., Vandenberg, L.N., 2018. CLARITY-BPA academic laboratory studies identify consistent low-dose Bisphenol A effects on multiple organ systems. Basic Clin. Pharmacol. Toxicol. 125 (3), 14–31.
Ratajczak-Wrona, W., Nowak, K., Garley, M., Grubczak, K., Dabrowska, D., Iwaniuk, A., Wilk, S., Moniuszko, M., Czerniecki, J., Wolczynski, S., Jablonska, E., 2019. Expression of serine proteases in neutrophils from women and men: regulation by endocrine disruptor bisphenol A. Environ. Toxicol. Pharmacol. 71, 103212.
Rizzo, A., Napoli, A., Roggiani, F., Tomassetti, A., Bagnoli, M., Mezzanzanica, D., 2018. One-carbon metabolism: biological players in epithelial ovarian cancer. Int. J. Mol. Sci. 19, 2092.
Rochester, J.R., 2013. Bisphenol A and human health: a review of the literature. Reprod. Toxicol. 42, 132–155.
Rodríguez-Marí, A., Cañestro, C., BreMiller, R.A., Catchen, J.M., Yan, Y.-L., Postlethwait, J.H., 2013. Retinoic acid metabolic genes, meiosis, and gonadal sex differentiation in zebrafish. PloS One 8, e73951.
Rone, M.B., Midzak, A.S., Issop, L., Rammouz, G., Jagannathan, S., Fan, J., Ye, X., Blonder, J., Veenstra, T., Papadopoulos, V., 2012. Identification of a dynamic mitochondrial protein complex driving cholesterol import, trafficking, and metabolism to steroid hormones. Molecular endocrinology (Baltimore, Md.) 26, 1868–1882.
Russo, G., Barbato, F., Mita, D.G., Grumetto, L., 2019. Occurrence of Bisphenol A and its analogues in some foodstuff marketed in Europe. Food Chem. Toxicol. 131, 110575.
Ryoo, I.-g., Kwak, M.-K., 2018. Regulatory crosstalk between the oxidative stress-related transcription factor Nfe2l2/Nrf2 and mitochondria. Toxicol. Appl. Pharmacol. 359, 24–33.
Sant, K.E., Timme-Laragy, A.R., 2018. Zebrafish as a model for toxicological perturbation of yolk and nutrition in the early embryo. Curr Env Hlth Rep 5, 125–133.
Segner, H., 2009. Zebrafish (Danio rerio) as a model organism for investigating endocrine disruption. Comp. Biochem. Physiol. C Toxicol. Pharmacol. 149, 187–195.
Shi, X.-Y., Wang, Z., Liu, L., Feng, L.-M., Li, N., Liu, S., et al., 2017. Low concentrations of bisphenol A promote human ovarian cancer cell proliferation and glycolysis-based metabolism through the estrogen receptor-α pathway, 2017. Chemosphere 185, 361–367.

Shukla, P., Mukherjee, S., 2020. Mitochondrial dysfunction: an emerging link in the pathophysiology of polycystic ovary syndrome. Mitochondrion 52, 24–39.
Singleman, C., Holtzman, N.G., 2014. Growth and maturation in the zebrafish, Danio rerio: a staging tool for teaching and research. Zebrafish 11, 396–406.
Steffensen, I.-L., Dirven, H., Couderq, S., David, A., D'Cruz, S.C., Fernández, M.F., Mustieles, V., Rodríguez-Carrillo, A., Hofer, T., 2020. Bisphenols and oxidative stress biomarkers-associations found in human studies, evaluation of methods used, and strengths and weaknesses of the biomarkers. Int. J. Environ. Res. Publ. Health 17, 3609.
Sugiura, K., Pendola, F.L., Eppig, J.J., 2005. Oocyte control of metabolic cooperativity between oocytes and companion granulosa cells: energy metabolism. Dev. Biol. 279, 20–30.
Sutton-McDowall, M.L., Gilchrist, R.B., Thompson, J.G., 2010. The pivotal role of glucose metabolism in determining oocyte developmental competence. Reproduction 139, 685–695.
Tebay, L.E., Robertson, H., Durant, S.T., Vitale, S.R., Penning, T.M., Dinkova-Kostova, A. T., Hayes, J.D., 2015. Mechanisms of activation of the transcription factor Nrf2 by redox stressors, nutrient cues, and energy status and the pathways through which it attenuates degenerative disease. Free Radic. Biol. Med. 88, 108–146.
Trapphoff, T., Heiligentag, M., El Hajj, N., Haaf, T., Eichenlaub-Ritter, U., 2013. Chronic exposure to a low concentration of bisphenol A during follicle culture affects the epigenetic status of germinal vesicles and metaphase II oocytes. Fertil. Steril. 100, 1758–1767 e1751.
Tugaeva, K.V., Titterington, J., Sotnikov, D.V., Maksimov, E.G., Antson, A.A., Sluchanko, N.N., 2020. Molecular basis for the recognition of steroidogenic acute regulatory protein by the 14-3-3 protein family. The FEBS Journal 287 (18), 3944–3966.
Tyanova, S., Temu, T., Cox, J., 2016a. The MaxQuant computational platform for mass spectrometry-based shotgun proteomics. Nat. Protoc. 11, 2301.
Tyanova, S., Temu, T., Sinitcyn, P., Carlson, A., Hein, M.Y., Geiger, T., Mann, M., Cox, J., 2016b. The Perseus computational platform for comprehensive analysis of (prote) omics data. Nat. Methods 13, 731–740.
Valentino, R., D'Esposito, V., Ariemma, F., Cimmino, I., Beguinot, F., Formisano, P., 2016. Bisphenol A environmental exposure and the detrimental effects on human metabolic health: is it necessary to revise the risk assessment in vulnerable population? J. Endocrinol. Invest. 39, 259–263.
Vandenberg, L.N., 2014. Non-monotonic dose responses in studies of endocrine disrupting chemicals: bisphenol a as a case study. Dose-Response 12, 259–276.
Veleri, S., Punnakkal, P., Dunbar, G.L., Maiti, P., 2018. Molecular insights into the roles of Rab proteins in intracellular dynamics and neurodegenerative diseases. NeuroMolecular Med. 20, 18–36.
Völkel, W., Colnot, T., Csanady, G.A., Filser, J.G., Dekant, W., 2002. Metabolism and kinetics of bisphenol A in humans at low doses following oral administration. Chem. Res. Toxicol. 15, 1281–1287.
Wang, Z., Wang, L., Zhang, Z., Feng, L., Song, X., Wu, J., 2019. Apolipoprotein A-IV involves in glucose and lipid metabolism of rat. Nutr. Metabol. 16, 41-41.
Warzych, E., Lipinska, P., 2020a. Energy metabolism of follicular environment during oocyte growth and maturation. J. Reprod. Dev. 66, 1–7.
Warzych, E., Lipinska, P., 2020b. Energy metabolism of follicular environment during oocyte growth and maturation. J Reprod Develop 66, 1–7.
Wells, L., Whalen, S.A., Hart, G.W., 2003. O-GlcNAc: a regulatory post-translational modification. Biochem. Biophys. Res. Commun. 302, 435–441.
Xie, H.-L., Wang, Y.-B., Jiao, G.-Z., Kong, D.-L., Li, Q., Li, H., Zheng, L.-L., Tan, J.-H., 2016. Effects of glucose metabolism during in vitro maturation on cytoplasmic maturation of mouse oocytes. Sci. Rep. 6, 20764-20764.
Xiong, Y., Bian, C., Lin, X., Wang, X., Xu, K., Zhao, X., 2020. Methylenetetrahydrofolate reductase gene polymorphisms in the risk of polycystic ovary syndrome and ovarian cancer. Biosci. Rep. 40, BSR20200995.
Yilmaz, O., Patinote, A., Nguyen, T., Com, E., Pineau, C., Bobe, J., 2019. Genome editing reveals reproductive and developmental dependencies on specific types of vitellogenin in zebrafish (Danio rerio). Mol. Reprod. Dev. 86, 1168–1188.
Yoon, S.Y., Kim, R., Jang, H., Shin, D.H., Lee, J.I., Seol, D., Lee, D.R., Chang, E.M., Lee, W.S., 2020. Peroxisome proliferator-activated receptor gamma modulator promotes neonatal mouse primordial follicle activation in vitro. Int. J. Mol. Sci. 21.
Zaidi, N., Swinnen, J.V., Smans, K., 2012. ATP-citrate lyase: a key player in cancer metabolism. Canc. Res. 72, 3709.
Zhang, J., Bao, Y., Zhou, X., Zheng, L., 2019. Polycystic ovary syndrome and mitochondrial dysfunction. Reprod. Biol. Endocrinol. 17, 67-67.
Zhu, H., Blake, S., Chan, K.T., Pearson, R.B., Kang, J., 2018. Cystathionine β-synthase in physiology and cancer. BioMed Res. Int. 2018, 3205125.